Université de Limoges

Faculté de Pharmacie

Ecole Doctorale Sciences Technologie et Santé

Laboratoire de Chimie Analytique et de Bromatologie

N° d'ordre :

THESE

Pour obtenir le grade de

DOCTEUR DE L'UNIVERSITE DE LIMOGES

Discipline : Chimie Appliquée

Présentée et soutenue publiquement par

James KASSAB

Le 6 Juillet 2004

Analyse et séparation de particules colloïdales et microniques par la méthode du Fractionnement par Couplage Flux Force à champ multigravitationnel

Sedimentation Field Flow Fractionation for the characterization of colloidal and micron particulate species

---

Directeur de Thèse : Professeur Philippe Cardot

Jury

Richard Zahoransky	Professeur, Fachhochschule Offenburg	Rapporteur
Alain Foucault	Maître de conférences HDR, GEPEA, Nantes	Rapporteur
Michael Claussen	Professeur, CUTEC Institut, Clausthal	Examinateur
Sergey P. Fisenko	Docteur S-Sciences, Luikov Institut, Minsk	Examinateur
Serge Battu	Maître de conférences HDR, LCAB, Limoges	Examinateur
Philippe Blanchart	Maître de conférences HDR, ENSCI, Limoges	Examinateur

A ma future épouse, Jocelyne / To my future wife, Jocelyne

A ma famille / To my family

A Père Joseph et tous ceux qui me sont chers /
To Father Joseph and all my dear ones

Remerciements-Acknowledgments

With a great adventure coming to an end, it seems to be a very suitable time to acknowledge those who contributed by their support and encouragement in the achievement of my thesis. It is of course impossible to mention all of you who have crossed my way during the last three years, so to all of those persons who are not mentioned below, thanks for the positive and supportive atmosphere that they provided me.

First of all I would like to express my deepest gratitude to my supervisor Prof. *Philippe Cardot* for accepting me in his laboratory as a Ph.D. student. He offered me the freedom in making my own choices and perspectives by sending me on a mission to Germany after a three month "military training" following a *Cardot's* special technique. A mission which was hard at the beginning and very successful at the end. I worked during these three years in a very autonomous way in order to satisfy my curiosity and explore my scientific capacities, but when needed he has always been there to support me. I thank him also for hosting me each time I traveled to Limoges.

I want to direct my gratitude to *Serge Battu* for his technical advices on SdFFF and his precious help with administrative stuff. Furthermore, I deeply appreciated his moral and human support when I was robed in Limoges. *Dominique Clédat* is thanked for her kindness and her contribution in one of the presented manuscripts. *Marie-Françoise Dreyfuss* as well as the other lab staff are also thanked for their sympathy and concern about my research work during these three years. *Philippe Blanchart* of ENSCI is gratefully acknowledged for his collaboration concerning the electron microscopy.

I also want to deeply acknowledge Prof. *Richard Zahoransky* who played a major role in the achievement of my thesis. Thanks to him, I was granted a fellowship in the years 2002 and 2003 by the German Academic Exchange Service (DAAD) through Offenburg's International Quality Network (IQN) "Nanoparticles and Biological Particles" project (NaBiPa). Therefore, I was invited to reside in Offenburg most of the time during the last three years. There, I had the opportunity to organize my research program. I appreciate also a lot the trust that he has in me by authorizing the use of the

available financial and technical means to fulfill my research tasks. He is to a large part "responsible" for where I am today.

I also would like to thank Prof. *Michael Claussen* and *Annett Wollmann* from CUTEC Institut GmbH for providing me with soot samples and for their interest about the fractionating potential of SdFFF in the analysis of soot particles. I really enjoyed my short visit to CUTEC even though it was raining all the time. Apparently, it rains there around 300 days per year and they are used to this. However, for Mediterranean guys like me, it will be hard to survive there. I also thank *Markus Maly* and his family for their kindness and sympathy. *Michael Lehmann* IQN's coordinator is gratefully thanked for his excellent administrative and friendship qualities. He was always there when I needed help and thanks to IQN, I managed to add the German language to my CV. *Juergen Meyer* the "Energy Conversion and Management" master program coordinator at Fachhochschule Offenburg (FHO), is acknowledged for his sympathy and for covering part of the printing expenses of my dissertation.

Prof. *Bernd Spangenberg*, head of the analytical chemistry department at FHO, is gratefully acknowledged first for providing me an appropriate and calm lab space to install my equipments and then for giving me the full access to the available chemical reagents and laboratory equipments when needed. Mr. *Rüdiger Hoffmann*, Frau *Rejina Brämer* and Frau *Andrea Seigel* are also thanked for their kindness and sympathy.

I was among the luckiest Ph.D. students who had the possibility to supervise some project works related to my research subject. I enjoyed being a nice friendly boss with time restricted targets to reach. Thanks to *Eduardo Pereira*, *César de Juan Esteban* and *Omar Valdés Solórzano* for their great job.

I would like to express my gratitude to *Berhart Schwarz* and *Clauss Bühler* at FHO for their valuable technical assistance. The electrical and mechanical workshops at FHO are also thanked for all provided and manufactured items. Thanks are also due to *Edgar Laile* of Wizard Zahoransky KG for his help on the laser detection technique.

Coming from cold Minsk-Belarus, Prof. *Sergey Fisenko*, formal guest professor at IQN, is thanked for his encouragement and new ideas about the FFF theory. Finally, a deep thought to my landlords *Hans*, *Helga*, *Michael* and *Torsten Conrad* for considering me as a true family member without forgetting their big and lovely dog *Ungschli*.

Table of contents

Preface

This report is a dissertation for a European doctorate in Applied Chemistry. The research work was fulfilled at the Faculty of Pharmacy (Université de Limoges, France) and the University of Applied Sciences (Offenburg, Germany).

The first part contains condensed background information on the subject of the thesis and a short overview with a general discussion about the main results presented in the manuscripts in the second part. The first part gives the necessary elements to scientists who are not active in this field to facilitate the reading of the second part. The second part is composed of manuscripts intended for publication in scientific journals. At the end, two technical reports are added as they describe some instrumentation achievements especially made in the frame of this research work.

This report is of interest for active scientists in the same field and easily understandable by students (with little or no experience in the field) who often tend to search for information on various practical issues in research articles. The content is diverse and well structured. It is also written with special attention to the minor practical details that seldom are mentioned in research articles.

Acronyms and Abbreviations

CPC	Condensation particle counter
CSPS	Coulter Sub-micron Particle Sizer
CV	Coefficient of variation
CVS	Constant volume sampling
DLS	Dynamic light scattering
DNA	Deoxyribonucleic acid
EAA	Electrical aerosol analyzer
EGR	Exhaust gas recirculation
EMG	Exponentially modified gaussian
FFF	Field-flow fractionation
GFFF	Gravitational FFF
HD	Heavy duty
HETP	Height equivalent to a theoretical plate
HPLC	High performance liquid chromatography
LD	Light duty
LMPE	Long path multi-wavelength extinction technique
MALS	Multi-angle laser light scattering
OMT	Optical multiwavelength technique
PAH	Polycyclic aromatic hydrocarbons
PCS	Photon correlation spectroscopy
PI	Polydispersity index
PLC	Programmable logic controller
PM	Particulate matter
PUI	Pump unit injection
RES	Raw exhaust gravimetric sampling
RPM	Rotation per minute
SdFFF	Sedimentation field-flow fractionation
SDP	Size distribution processor
SEM	Scanning electron microscopy
SMPS	Oline-scanning mobility particle sizer
SMS	Scanning mobility analyzer
TOF-MS	Time-of-flight mass spectrometry
UV/Vis	Ultraviolet/visible
VGT	Variable geometry toroidal
VW	Volkswagen

List of symbols

$\langle v \rangle$	Mean cross-sectional velocity of the carrier liquid
η	Fluid viscosity,

δ	Shortest distance of the particle from the accumulation wall
μ	Electrophoretic mobility
a	Particle radius
c	Concentration of the solute
C_V	Dimensionless volume concentration
D	Diffusion coefficient
d	Particle diameter
$\Delta\rho$	Density difference between the particle and carrier
d_i	Steric inversion diameter
DQ	Dispersion quotient DQ
D_T	Coefficient of thermal diffusion
F	Centrifugal force
f	Friction coefficient
F_L	Hydrodynamic lift forces
G	Centrifugal acceleration
G_A	Particle Archimedes weight
I	Attenuated light intensity
I_0	Initial light intensity,
j	Flux of the solute
k	Boltzmann constant
L	Channel length
l	Mean layer thickness
λ	Light wavelength
M	Molecular weight
m'	Effective particle mass,
n	Effective refractive index
N	Particle number density
N	Plate number
$p(r)$	Size distribution
ρ	Particle density
Q_{ext}	Extinction coefficient,
r	Particle radius,
R	Retention ratio
s_0	Undisturbed shear rate at the accumulation wall
S_d	Size based selectivity S_d,
T	Absolute temperature
t_0	Void time
α	Thermal diffusion coefficient
t_r	Retention time
U	Velocity vector induced by the external field,
v	Resulting velocity vector
V	Velocity vector induced by the flow
V_P	Particle volume
w	Channel thickness,
X	Data points
γ	Perturbation factor

List of manuscripts

This thesis is based on results presented in the following manuscripts submitted to scientific journals and referred to in the summary by their roman numerals.

I. Comparative size determination of latex and oxide particles by optical multiwavelength technique, photon correlation spectroscopy and scanning electron microscopy

James R. Kassab, Richard A. Zahoransky, Philippe Blanchart, Dominique Clédat, Philippe J.P. Cardot

Analytica Chimica Acta, submitted.

II. Characterization of titanium and zirconium oxide colloids by off-line hyphenation of sedimentation field flow fractionation with optical multiwavelength technique

James R. Kassab, Richard A. Zahoransky, Philippe Blanchart, Philippe J.P. Cardot, Bernd Spangenberg

Journal of Colloid and Interface Science, will be submitted.

III. Size analysis of soot particles emitted from a light duty diesel engine using sedimentation field flow fractionation.

James R. Kassab, Annett Wollmann, Richard A. Zahoransky, Michael Claussen, Philippe J.P. Cardot

Analytical Chemistry, will be submitted.

IV. Fast "hyperlayer" separation development in sedimentation field flow fractionation using channels of reduced thickness.

James R. Kassab, Philippe J.P. Cardot, Richard A. Zahoransky, Serge Battu

Journal of Chromatography A, submitted.

The following paper is not included due to the nature of the material or the extent of my contribution

Particle emissions of the Jing-Cast burner examined by multi-wavelength particle analyzer.
Richard A. Zahoransky, Sven. Kerzenmacher, Guillaume Benali, Raphael Lavigne, James R. Kassab, Dale Henneke, Edgard Laile.
SAE Techn. Paper Series, 2003, No:2003-01-53

The author's contributions to the different manuscripts

Manuscript I. The author did all experimental work as well as data evaluation. The author wrote also the manuscript.

Manuscript II. The author conceptualized the hyphenation set up. He did all experimental work as well as data evaluation and he wrote the manuscript.

Manuscript III. The author made all the experiments except for sample collection and SMPS analysis. The author wrote the manuscript assisted by the second co-author.

Manuscript IV. The author made part of the experimental work and data evaluation. He prepared the substantial part of the manuscript.

Résumé

Le principe de séparation par la méthode du fractionnement par couplage flux-force (FFF) est basé sur l'action simultanée de l'écoulement d'un liquide dans un canal de faible épaisseur et l'effet d'un champ externe appliqué perpendiculairement au canal. Le champ d'application de cette technique est très large avec une étendue en taille allant du submicronique à des particules de plus de 100 µm. De nouvelles améliorations et modifications instrumentales sont apportées au prototype de FFF opérant à champ multigravitationnel (SdFFF) utilisé dans ce travail de recherche. Une séparation à champ multigravitationnel programmé a été explorée dans l'analyse de taille de suspensions colloïdales diverses en taille et densité telles les particules oxydées et celles des aérosols de diesels. Une seconde séparation à effet de focalisation plane par effet de paroi a été effectuée sur des particules de latex microniques en utilisant des canaux de faibles épaisseurs visant la minimisation du volume mort, le facteur de dilution ainsi que le temps de rétention et la consommation de phase mobile. En outre, une nouvelle technique de détection optique à multi longueurs d'onde (OMT) est présentée tout d'abord séparément dans une étude d'analyse de taille de diverses suspensions particulaires et ensuite dans un couplage « off-line » avec la SdFFF. Les résultats obtenus sont prometteurs et intéressants pour l'analyse de taille des espèces particulaires fractionnées par la FFF.

Abstract

The particle separation in field flow fractionation (FFF) is based on the combined action of a carrier liquid flowing through a thin, ribbonlike channel and an external field applied perpendicularly to the channel. The particle size range that can be separated is very broad ranging from a few nanometers to 100 µm, covering the entire colloidal, polymeric and even most of the micron particle domain. Sedimentation field flow fractionation (SdFFF) operating at multi gravitational field is the separating technique used in this research work. This thesis describes the further evaluation and development of SdFFF systems. A field programmed separation is explored in size analysis of colloidal suspensions such oxide and soot particles. A fast hyperlayer separation of latex micron particles is also performed using channels of reduced thickness which aims are to reduce the channel void volume, dilution factor, as well as elution time and mobile phase consumption. Furthermore, a detection technique called optical multiwavelength technique (OMT) is newly introduced alone first in a study for size analysis of particle suspensions with different complexity and then in off-line hyphenation with SdFFF which promising results are of a great interest for fractionated particulate samples by FFF.

Introduction

Field Flow Fractionation (FFF) is a family of flexible analytical fractionating techniques which have the great advantage that separation is achieved through the interaction of the sample with an external physical field and without a stationary phase. This has the advantage of avoiding the large variety of problems due to non-specific sample interactions with column materials associated with other chromatographic techniques. Furthermore, the range of information accessible is very broad and often complimentary when various FFF techniques are applied, so that even very complex systems with broad size distribution, heterogeneous mixtures or strongly interacting systems can be characterized. The particle size range that can be separated is very broad ranging from a few nanometers to 100 µm, covering the entire colloidal, polymeric and even most of the microparticle domain. No other technique can cover about 5 orders of magnitude of the particle size, even with complex distributions.

This thesis introduces the basic separation principle of FFF and an overview on the most relevant subtechniques focusing on sedimentation FFF (SdFFF) used in this research work. It describes also the latest instrumentation developments made on our SdFFF system: i) the field programming applied to the separation of broadly distributed colloidal particulate samples; ii) the use of channels of reduced thickness to reduce the channel void volume, dilution factor, as well as elution time and mobile phase consumption. The performance of these channels is tested on standard latex micron particles. Furthermore, a new detection set up is introduced, called optical multiwavelength technique (OMT). It is a particle measurement technique developed for suspensions and aerosols based on the Mie theory. It delivers in on-line/in-line mode the particle mean size and volume concentration over an entire particle population. OMT is still unknown among other detection techniques used in the FFF domain. Its performance has been mostly demonstrated in applications of size analysis of dispersed particles in aerosols. However, it is not yet well investigated on particulate matter in suspension. In this report, OMT's performance is firstly explored in size analysis of suspended particles with different complexity and then in off-line hyphenation with SdFFF. Promising results are obtained from applications for size analysis of fractions collected from various colloids.

Field Flow Fractionation (FFF)

1. Historical introduction

Field flow fractionation (FFF) was first conceptualized in the 1960s by J.C. Giddings [1-3] and has since then evolved into a number of subtechniques [4, 5]. Species can be separated in the 10^5-fold size range from 10^{-3} to 10^2 µm. The separation is carried out inside a thin, ribbonlike flow channel (Figure 1). This channel is composed of a thin piece of sheet material (usually 70-300 µm thick Mylar or polyimide) in which a channel is cut and clamped afterwards between two walls of highly polished plane parallel surfaces.

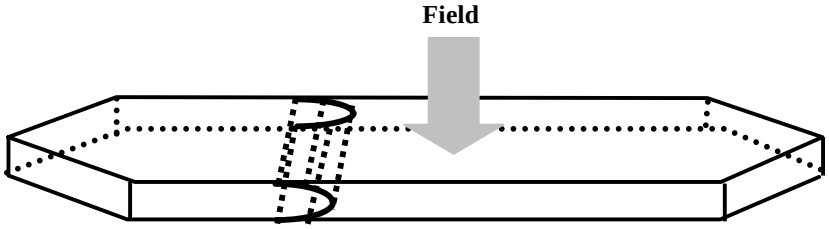

Figure 1. Schematic representation of an FFF channel.

Common to all FFF subtechniques is the establishment of a laminar flow with a parabolic profile in the volume of the channel, as a carrier liquid is pumped through. Samples components are eluted from the channel at certain retention times but unlike chromatography, the retention of sample components is caused by an external field applied perpendicular to the flow (Figure 1). This field interacts with the sample components and concentrates them against one of the channel walls, called the accumulation wall. The retention times in FFF are related to various physicochemical properties of the retained species. These physicochemical properties (Table 1) can be determined from the measured retention times depending on the FFF subtechnique used.

Table 1. Physicochemical properties of solutes in the commonly used FFF subtechniques

FFF subtechnique	Physicochemical property[a] controlling the retention
Sedimentation FFF	M, D, ρ, d
Flow FFF	D, d
Thermal FFF	α, D_T
Electrical FFF	D, μ

[a] Symbols: M: Molecular weight; ρ: density; D: diffusion coefficient; d: diameter; α: thermal diffusion coefficient; D_T: coefficient of thermal diffusion; μ: electrophoretic mobility

2. Most used FFF subtechniques

Over the years, several fields have been used in FFF instead of a single universal field because the different field types have different ranges and areas of applicability. Therefore, several subtechniques have been developed. Some are more successful than others due to the instrumentation complexity or the nature of macromolecular or particulate sample under investigation. The most commonly used FFF subtechniques are thermal, electrical, flow and sedimentation FFF. Thermal and flow FFF are largely used in polymer analysis, of which thermal FFF is used for polymer analysis in organic solvents and flow FFF in aqueous solvents [6]. Flow FFF has on occasion been used for polymer analysis in organic solvents [7, 8]. Flow FFF is commonly used in one of three variants, symmetrical, asymmetrical or hollow fiber flow FFF. The subtechnique used in the present work is the sedimentation FFF (SdFFF) and the discussion will therefore be limited to that, although some of the principles and discussions will also apply to FFF in general. A brief introduction to SdFFF is given below. For a presentation of the other FFF subtechniques, the reader is referred to a selection of articles and books [9-16].

3. Sedimentation field flow fractionation (SdFFF)

SdFFF uses a sedimentation field at right angles to the channel flow. The earth gravity is the simplest sedimentation field that can be used. This technique, known as gravitational FFF, is not difficult and expensive to build. It is suitable for the separation of rather large particles (> 1 µm in diameter) and has been used in the analysis of blood

cells [17, 18], yeast [19] and stem cells [20]. For SdFFF, stronger fields are applied. Therefore, the channel is coiled inside a centrifuge rotor basket (Figure 2). The field strength is monitored by the rotation speed.

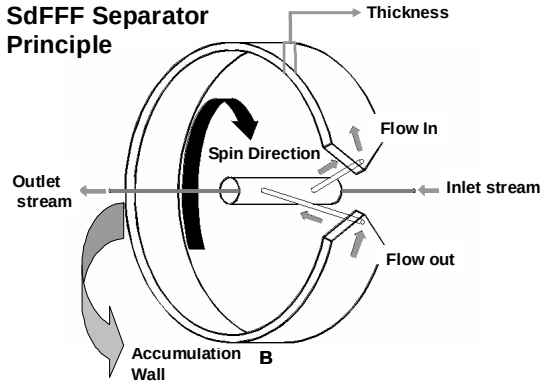

Figure 2. Schematic representation of the channel coiled inside the rotor basket. The channel is spun at different rotation speeds, thereby controlling the sedimentation field strength.

Samples components are separated according to their size and density. The centrifugal force [21] applied on spherical particles can be given by several forms:

$$F = m' \cdot G = V_P \cdot |\Delta\rho| \cdot G = \frac{\pi}{6} \cdot d^3 \cdot |\Delta\rho| \cdot G \qquad (1)$$

where *m'* is the effective particle mass, V_P the particle volume, $\Delta\rho$ the density difference between the particle and carrier, *G* the centrifugal acceleration, and *d* the particle diameter.

The first SdFFF system was commercially available since the mid eighties. The instrumentation for SdFFF is complex and expensive because of the need for a centrifugal apparatus with special rotating seals. Despite its broad applicability and high separating effectiveness, the usage of SdFFF became limited because of several instrumentation problems that were found on the commercial system. Cardot et al. are nowadays the only team who is mainly active in SdFFF instrumentation and applications. Another system with a new design was developed and since several modifications were continuously made. Its performance was demonstrated in several applications [22-25]. After its first

introduction by Giddings, SdFFF was used for the fractionation of industrial colloids [26] and environmental material [27]. It proved mostly its utility in biological applications, such as the analysis of proteins [28], viruses [29, 30], liposomes [31], DNA [32, 33], yeast [34], different cell organelles and fragments [35, 36] as well as stem [37] and whole cells [38].

4. Theory of retention

4.1. Retention in the normal mode

A carrier liquid is pumped through the channel from the inlet (Figure 2), where the sample is injected, to the outlet, to which a detector is connected. Inside the channel, a parabolic flow profile (laminar Newtonian flow) is established as in a capillary tube. Thus, flow velocities vary from zero at the walls to a maximum in the center of the channel. While the carrier liquid with the sample is flowing through the channel, an effective physical field (the sedimentation force in case of SdFFF) is applied across the channel perpendicular to the flow direction of the carrier liquid. Interaction with the field concentrates the solute at the accumulation wall. The gravity center of the solute zones lies very near to the wall (Figure 3A), usually extending only a few micrometers. Due to the established concentration gradient, a diffusion flux in the reverse direction is included according to Fick's law. After a short time a steady state is reached, and the exponential distribution of the solute cloud across the channel can be described by a mean layer thickness *l*. Due to the parabolic flow velocity profile, the solutes are transported in the direction of the longitudinal channel axis at varying velocities, depending on their distance from the channel walls. The nearer the solute is located to the accumulation wall, the later it will elute. Since smaller particles (1) diffuse faster than larger ones (2) and so they establish a higher layer thickness *l*, the elution sequence proceeds from the smaller solutes to the largest ones (Figure 3A). Hence, the flow velocity profile of the carrier liquid amplifies very little distance differences between the solute clouds in the x-

direction, leading to the separation. This elution mode is the classical one in FFF called normal or Brownian mode.

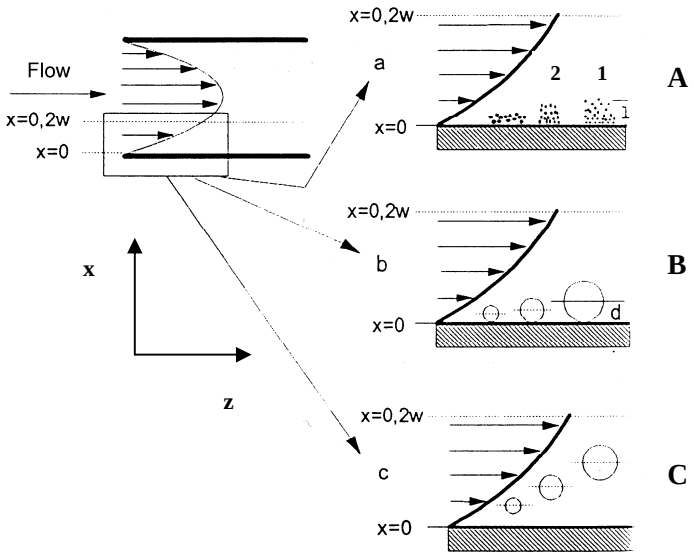

Figure 3. Schematic representation of the different elution modes : normal/Brownian (A), steric (B) and steric hyperlayer (C).

The retention in FFF can be mathematically described by the pseudo-equilibrium theory [39]. The solute is displaced in a moving fluid by the combined action of the flow and the applied external field. The resulting velocity vector *v* can be decomposed into two perpendicular vectors: *U*, induced by the applied field, and a flow-induced component v:

$$v = U + \mathrm{v} \tag{2}$$

The flux of the solute *j* can also be written as the sum of the two axial components in the direction of the flow (z) and the direction of the field (x):

$$j = j_x + j_z \tag{3}$$

According to Fick's law, the axial components of the flux can be expressed by:

$$j_x = -D_x \frac{dc}{dx} + U.c \qquad \text{and} \qquad j_z = -D_z \frac{dc}{dx} + \mathrm{v}.c \tag{4}$$

where D_x and D_z are the diffusion coefficients and *c* the concentration of the solute. With Eq. 4, another equation describing the concentration profile of a particle cloud of a solute along the x axis can be deduced:

$$c = c_0 \cdot \exp\left(\frac{-x \cdot |U|}{D}\right) \tag{5}$$

where c is the concentration of the solute at distance x from the accumulation wall (Figure 3A), c_0 the concentration of the solute at the accumulation wall. As U and D are size and density dependent factors, Eq. 5 describes the concentration profile of particles depending on their size and density. The mean layer thickness l is introduced as a characteristic parameter for such particles. l is defined as:

$$l = \frac{D}{|U|} \tag{6}$$

Eq. 5 can be thus rewritten as:

$$c = c_0 \cdot \exp\left(\frac{-x}{l}\right) \tag{7}$$

The mean layer thickness l depends on the force F exerted on the solute as shown by the following equations:

$$U = \frac{F}{f} \quad \text{and} \quad D = \frac{k \cdot T}{f} \quad \text{yield} \quad l = \frac{k \cdot T}{|F|} \tag{8}$$

where f is the friction coefficient, k the Boltzmann constant and T the absolute temperature.

The so-called standard model for the Brownian mode retention assumes that all particles are noninteracting point masses. The velocity v of a particle cloud is simply the average velocity of an exponential distribution embedded in a parabolic flow profile. The velocity v within the parabolic flow profile is distributed across the x-axis according to the expression:

$$v = 6 \cdot \langle v \rangle \cdot \left[\frac{x}{w} - \left(\frac{x}{w}\right)^2\right] \tag{9}$$

where $\langle v \rangle$ is the mean cross-sectional velocity of the carrier liquid and w the channel thickness. The position of the gravity center of a particle cloud is its l value. The higher the position of the gravity center in the channel thickness, the faster the cloud moves (Figure 3A).

In FFF, the retention ratio R of particles is described by the ratio of their displacement velocity to the mean cross-sectional velocity of the carrier:

$$R = \frac{v}{\langle v \rangle} \tag{10}$$

R is also given by:

$$R = \frac{t_0}{t_r} \tag{11}$$

where t_0 is the void time, i.e. the elution time of a non-retained tracer and t_r the retention time. t_r is the ratio of the channel length L to the mean cross-sectional velocity $\langle v \rangle$:

$$t_r = \frac{L}{\langle v \rangle} \tag{12}$$

R is found to be related to the l/w ratio of a particle cloud by [40]

$$\frac{t_0}{t_r} = R = \frac{6 \cdot l}{w}\left[\coth\frac{w}{2 \cdot l} - \frac{2 \cdot l}{w}\right] \tag{13}$$

Eq. 13 is a basic theoretical relationship that describes quantitatively the retention in the Brownian mode.

When $w >> l$, R is approximated by

$$R = 6 \cdot \frac{l}{w} \tag{14}$$

In the Brownian mode, the diffusion coefficient D is not negligible. It decreases with an increasing particle size or mass. This means that larger particles move closer to the accumulation wall than smaller ones because of their weaker Brownian movement, which is opposed to the external field. Consequently, smallest particles elute first.

4.2. Retention in the steric and steric-hyperlayer modes

If the intensity of the external field (the sedimentation force in case of SdFFF) is high enough to press all the solutes as close as possible to the accumulation wall of the channel (Figure 3B), another elution mode becomes operative, called steric mode. Giddings and Myers [41] in 1978 showed that the elution order is inverted for particles

with a diameter larger than 1 µm, i.e. bigger particles are eluted before smaller ones. The transition region can be experimentally determined by plotting the retention time t_r versus the particle diameter d as illustrated in Figure 4. In the Brownian mode, the retention time increases with the particle diameter d until it reaches the steric inversion diameter $d_i \cong 1$ µm which is the upper limit of the Brownian mode operation. In the steric mode, applicable to larger particles, the retention time increases with a decreasing diameter until $d = d_i$ [41]. For samples with a broad size distribution in the micron range, it is important to avoid the transition region between the normal and the steric mode during the measurement. This can be achieved by proper adjustment of the channel thickness, channel flow and the strength of the applied field [42].

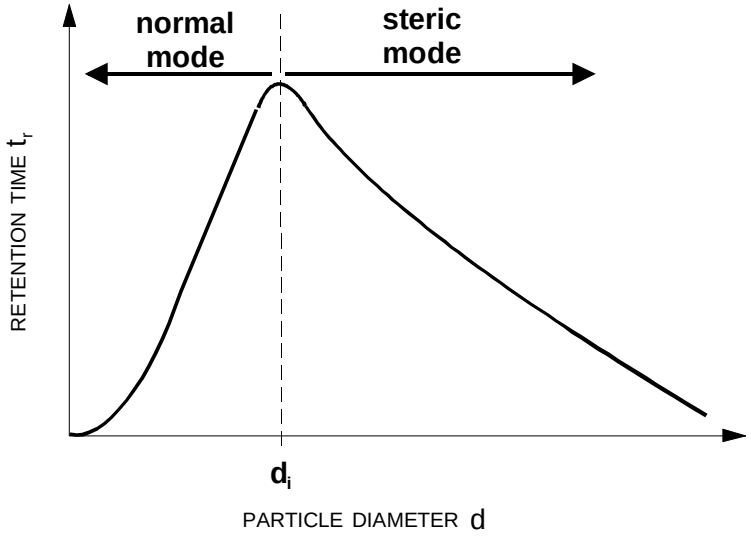

Figure 4. Steric inversion diameter d_i; this plot is valid only for particles of equal density and shape.

A theoretical retention model based on steric exclusion was developed. Solid spherical particles execute Brownian movements within a channel width of $w - 2 \cdot (a/w)$, where a is the particle radius. From Eq. 14, the retention ratio R in the steric mode can be approximated [43] by

$$R \cong 6 \cdot \frac{a}{w} + 6 \cdot \frac{l}{w} \qquad (15)$$

For particles in the micron size range, the diffusion coefficient D is very small. The second term of Eq. 15 becomes negligible. The first term corresponds to the movement of a particle rolling on the channel accumulation wall. Eq.15 is simplified to the form:

$$R \cong 6 \cdot \frac{a}{w} \tag{16}$$

In contrast to the Brownian mode, the retention ratio R increases with an increasing particle size. The steric model describes an ideal case of elution where particles are forced into a thin uniform layer at the accumulation wall and move along the channel forced by the carrier liquid flow. The protrusion of the particles into the flow stream is determined by their physical size. The gravity center of larger particles moves in faster flow streams (Figure 3B). The migration velocity increases with the particle diameter.

In this model, R is only dependent on the particle diameter and the channel thickness. Unfortunately, this could be hardly observed experimentally. There are a number of influences that cause perturbations of the retention. To account for these influences, a factor $\gamma$is added to Eq. 16:

$$R \cong 6 \cdot \gamma \cdot \frac{a}{w} \tag{17}$$

The presence of viscous drag, for example, leads to a particle rotation and reduces the migration velocity of the particles [44]. In this case γ is smaller than unity. The retention can also be reduced by various particle-wall and particle-particle interactions. Some of these interactions were investigated by Reschiglian et al. [45].

As the average velocity of the carrier in the channel increases, particles that are in close contact with the accumulation wall experience hydrodynamic lift forces. These forces move the particles into a confined region from the wall that is thin relative to their size, or focused, as shown in Figure 3C. This is the basis of another elution mode called steric-hyperlayer mode [46] which is characterized by a high resolution in very short analysis times.

The existence of lift forces was discovered by Caldwell et al. [44]. In the steric-hyperlayer elution mode, the micron particles are driven away from the accumulation wall by hydrodynamic lift forces F_L and protrude into faster flow streams. They are forced into thin layers at an equilibrium position in the channel thickness where the

external field (sedimentation field in case of SdFFF) is balanced by the opposite hydrodynamic lift forces F_L. As the micron particles move in faster streamlines they elute earlier than predicted by Eq. 16 and γ becomes greater than unity. The factor γ for monodisperse, well characterized micron species has been found to increase with the channel flow velocity and decrease with an increasing field strength. The particles reach an equilibrium position, where the lift forces counterbalance the force exerted by the external field. For SdFFF, the external field is the gravitational field. F_L can be then written as:

$$F = F_L = \frac{\pi}{6} \cdot d^3 \cdot \Delta\rho \cdot G \tag{18}$$

Several approaches have been made to describe the hydrodynamic lift forces. Williams et al. [47] made retention measurements of latex microsphere standards by SdFFF and evaluated the results by multiple linear regression analysis. The following equation describing F_L, based on the lubrication phenomena, was obtained:

$$F_L = C \cdot \frac{a^3 \cdot \eta \cdot s_0}{\delta} \tag{19}$$

where η is the fluid viscosity, a is the particle radius, s_0 the undisturbed shear rate at the accumulation wall, δ the shortest distance of the particle from the accumulation wall and C a dimensionless coefficient whose value was approximated to 0.0075.

The model of Pazourek and Chmelík [48], based on inertia considerations, suggests another description for the lift forces based on the Navier-Stokes equation:

$$F_L = -\frac{81}{4} \cdot \pi \cdot \rho \cdot \langle v \rangle^2 \cdot \frac{a^4}{w^2} \cdot (1-2\delta) \cdot \left[\frac{K^2 - (1-2\delta)^2}{1-K} \right] \tag{20}$$

where $K = 0.62$, ρ the density of the carrier liquid and δ the dimensionless distance of the particle from the accumulation wall. The lift force function in Eq. 20 is displayed in Figure 5. The major consequence of the existence of such forces is that a given particle in the channel migrates downwards or upwards until it is focused at a vertical position δ where the magnitude of F_L equals the particle Archimedes weight G_A. These positions can be illustrated by the points of intersection of a straight line of the constant function G_A with the lift forces curve. It is noticed that there are three intersection positions. Figure 5 also shows that the lift force F_L changes its sign depending on the particle

position in the channel, and that there are three positions where F_L is equal to zero. The experimental results obtained by Pazourek and Chmelík show that this theoretical model is applicable if $\delta >> a/w$.

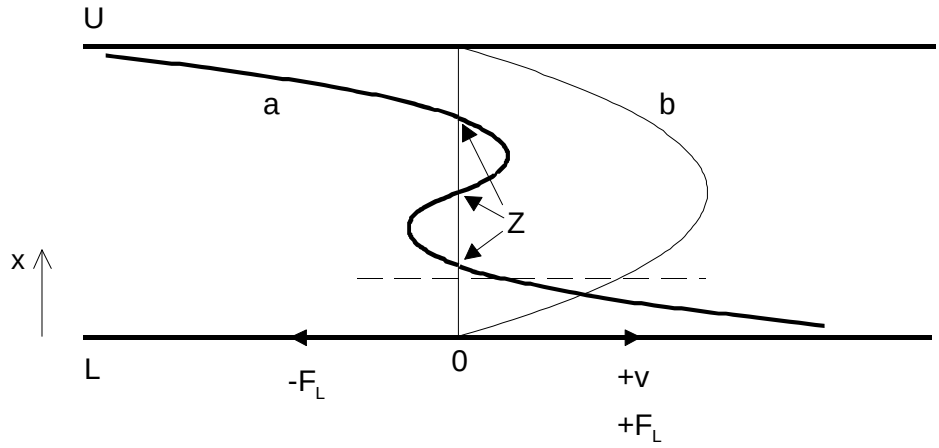

Figure 5. Schematic representation of the lift force function in a GFFF channel. U and L represent the upper and lower channel walls, curves a and b represent the courses of the lift forces and flow velocity profile respectively, $-F_L$ and $+F_L$ show the orientation of the lift forces and +v shows the direction of the carrier liquid flow. Z denotes three positions inside the channel where $F_L = 0$.

5. FFF and colloids

Colloids gained over the years a great interest in industrial and academic researches as they revealed their utility in a wide range of industrial applications. Part of the colloids concerned in this study were the titanium (TiO_2) and zirconium (ZrO_2) oxides. TiO_2 powder is widely used as a pigment or ceramic material because of its inert chemical properties and high refractive index. When it is used as a white pigment, properties depend on the scattering of light from small particles embedded in a transparent medium and then, the diffuse reflectance is a function of the grain distribution [49]. For ceramics, the sintering of the fine grained microstructure is particularly controlled by the grain size distribution and their aspect ratio. Sintered ceramics with well define pore structure can be used for sub-micron filtering [50]. In general, many powder formulations are under the form of disperse systems such as colloidal suspensions for which the stability is governed by the material itself and the liquid, but also by the grain size distribution [51]. A theoretical description of particle dispersion in a liquid can be

approached through models including parameters as the grain size. For example, it was shown that the dielectric properties at high frequency of concentrated TiO_2 suspensions [52] could be characterized using well known sub-micron particles.

Zirconia (ZrO_2) has a high melting point (2700° C) and a low thermal conductivity. For over 50 years, on-going research and development programs undertaken at various universities worldwide have produced new ideas on the industrial applications of ZrO_2. The science of catalysis has benefited enormously from these recent efforts. A host of reactions are now routinely catalyzed by zirconia powder including: polymerization, oxidation, hydrogenation, isomeration, environmental, autocatalysis, reduction and reforming. In addition to the catalysis applications, ZrO_2 is widely used also as a grinding media and engineering ceramics due to its increased hardness and high thermal shock resistance. Wear parts in automotive engines, thermal barrier coatings on jet engines and filters for molten metal are just three examples of products manufactured from zirconia powder. ZrO_2 is also used in applications such as oxygen sensors and solid oxide fuel cells due to its high oxygen ion conductivity. Other applications using ZrO_2 include paper coatings, electronic ceramics and glass (toughening and optical property control).

The other colloidal species concerned in this study are very different than oxide colloids as they are considered among the main sources of environmental pollution. Known by their intensive black color, low molecular weight and small grain size, soot particles are of a great concern for environmental and health researches as they revealed their effect on human mortality in big cities. Particulate emissions generated by combustion, represent a problem which continues to draw a significant attention worldwide [53] not only due to increasingly tighter environmental legislation but also due to very recent findings correlating mortality rates in cities [54] with concentrations of fine particles smaller than approximately 2.5 microns, most of which come from combustion sources. The particulate matter (PM) can cause serious health problems by penetrating and delivering coated chemicals into human respiratory systems [55, 56]. Current regulations are mainly concerned on the total PM amount, not the size of the particles. Although the size of soot particles is not regulated by national or international laws yet, its importance has grown up in the last years with the upcoming discussion of health effects caused by small particles. Diesel engines are considered to be the major source of particulate emission.

PM in automobile exhaust is mostly fine carbonaceous particles (soot) that are coated with a mixture of various toxic chemicals such as polycyclic aromatic hydrocarbons (PAH). Soot particles have irregular shapes (usually in chain forms) formed by aggregation of several primary spherical particles [57]. As the danger of soot increases as the particle size decreases, there have been an increasing number of studies on particle formation and PM emission of diesel engines [58-60].

Colloids were the first particulate species to be characterized by thermal FFF [61]. Since, they were subject of several systematic studies made by various FFF subtechniques including SdFFF which was applicable to the separation of a large variety of colloids [4, 29, 62, 63]. Studies have been made on their aggregation [64] and polydispersity [65], the mobile phase effect [45], the different particle-particle and particle-channel wall interactions [66], the relaxation procedure and the effect of the sample concentration [67]. Colloids are particles with a mean grain size generally smaller than one micron. Therefore, the elution mode of these particles is expected to be Brownian [15] as already demonstrated with other SdFFF techniques operated at high or moderated multi-gravitational fields [23, 68]. Beside their impact on industry and environment, oxide colloids and soot particles were also characterized in this work for other instrumentation purposes. One of these is to test the performance of our SdFFF system using an exponentially programmed separation. Oxide colloids are firstly separated with a good peak resolution at relatively low sedimentation fields due to their high density values. Soot particles are also separated with a remarkable resolution and repeatability. It is the first time that this biocompatible system is set to run at highly programmed field separation and its performance proved that it is at least equivalent to other commercial SdFFF systems. The second purpose for choosing oxide colloids and soot particles is to demonstrate the performance of the newly established off-line hyphenation of OMT with SdFFF in the size determination of time dependent eluted fractions.

Optical Multiwavelength Technique (OMT)

Most detection techniques for liquid chromatography are also used in FFF such as UV/Vis [69, 70] and photodiode array spectrophotometers [71], refractive index [8, 23, 72], viscometric [73], low and multi-angle laser light scattering (MALS) [74, 75-77] detectors and many others. For a deep insight of these detection techniques, the reader is referred to a number of articles and textbooks [15, 16, 78-81]. Only the optical multiwavelength technique (OMT) is presented in this report.

1. Measurement principle

OMT is a newly introduced particle measurement technique developed for aerosols and suspensions. It has been till now mostly used for particle emission applications [82-86]. However, it is not yet well investigated on particulate matter in suspension. OMT delivers in on-line/in-line mode the mean particle size and concentration. It applies the integral extinction of laser light beams of different wavelengths directed through particle loaded fluids (aerosols or suspensions). It enables measurements of particle collectives in the size range from 0.010 to 7 μm approximately depending on their refractive index. Particles in the measurement volume attenuate the light beam in consequence of scattering and absorption (Figure 6).

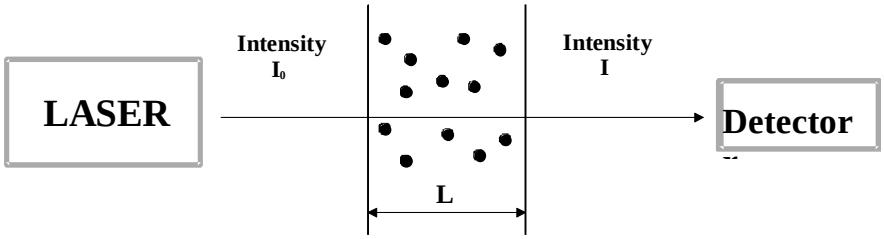

Figure 6. The measurement principle set up where I_0 is the initial intensity of the laser beam, I is the attenuated intensity and L is the optical path length of the measurement volume containing the particles.

With the definition of an extinction coefficient Q_{ext}, depending on the particle size, the effective refractive index ($n_{particle}/n_{medium}$) and the light wavelength, the integral intensity

attenuation can be described by Bouguer's law for monodisperse particle systems as follows:

$$I = I_0 \exp\{-N \cdot L \cdot \pi \cdot r \cdot Q_{ext}(r, \lambda, n)\} \tag{21}$$

where I is the attenuated intensity, I_0 the initial intensity, N the particle number density (number of particles per volume unit), L the optical path length, r the particle radius, Q_{ext} the extinction coefficient, λ the light wavelength and n the effective refractive index [82, 87]. If the intensity is measured by two light beams of different wavelengths, a dispersion quotient DQ can be formed, which depends only on the extinction coefficient and thus on the particle radius r and the effective refractive index n when two different wavelengths λ_1 and λ_2 are given:

$$DQ = \frac{\ln\left(\frac{I}{I_0}\right)_{\lambda_1, n}}{\ln\left(\frac{I}{I_0}\right)_{\lambda_2, n}} = \frac{-N \cdot L \cdot \pi \cdot r}{-N \cdot L \cdot \pi \cdot r} \times \frac{Q_{ext}(r, \lambda_1, n)}{Q_{ext}(r, \lambda_2, n)} = \frac{Q_{ext}(r, \lambda_1, n)}{Q_{ext}(r, \lambda_2, n)} \tag{22}$$

By measuring DQ, the particle radius r is obtained independently from N which is then calculated according to Eq. 21 at one of the wavelengths with the resulting radius from Eq. 22. The dimensionless volume concentration C_V is directly derived from N. C_V is defined as the volume taken by spherical particles with volumetrically averaged radius r_v related to the total volume.

Eq. 21 and 22 are valid for monodisperse particles. Thus, the analysis of polydisperse particle collectives requires the integration over the particle size distribution and Eq. 21 is converted to:

$$I = I_0 \cdot \exp\{-N \cdot L \cdot \pi \cdot \int_0^\infty p(r) \cdot r^2 . Q_{ext}(r, \lambda, n) dr\} \tag{23}$$

Consequently, Eq. 22 converts to:

$$DQ = \frac{\int_0^\infty p(r).r^2.Q_{ext}(r,\lambda_1,n)dr}{\int_0^\infty p(r).r^2.Q_{ext}(r,\lambda_2,n)dr} \quad (24)$$

where *p(r)* is the size distribution. The log-normal size distributions is assumed to be suitable for most applications:

$$p(r) = \frac{1}{\sigma_g \cdot r \cdot \sqrt{2\pi}} \cdot \exp\left(\frac{-[\ln(r) - \ln(r_g)]^2}{2\sigma_g{}^2} \right) \quad (25)$$

where r_g is the geometrical mean radius of the size distribution:

$$r_g = \sqrt[N]{\prod_{i=1}^{N} r_i} \quad (26)$$

r_i is the radius of an individual particle and σ_g is the geometrical standard deviation given by:

$$\sigma_g{}^2 = \int_0^\infty \{\ln(r) - \ln(r_g)\}^2 \cdot p(r)dr \quad (27)$$

The extinction coefficient Q_{ext} is calculated for spherical particles by the Lorentz-Mie theory [88, 89]. However, ambiguous results in the interesting size range may be obtained, particularly for absorbing particles. This is eliminated by using three different wavelengths. The third wavelength is furthermore a valuable tool to detect measurement errors caused by instrumental or operational errors like misestimating some theoretical parameters such as particle refractive indexes (real and imaginary), the size distribution range or the size standard deviation. By using a third wavelength, two independent dispersion quotients $DQ_1(\lambda_1, \lambda_2)$ and $DQ_2(\lambda_2, \lambda_3)$ can be calculated.

2. Parameter diagrams

For every type of particles in aerosols or in suspensions, a *DQ1-DQ2* parameter diagram is calculated by the system according to the Mie theory after the definition of certain experimental parameters related to the type of particles and their medium. These

parameters include the expected size range, the three laser wavelengths values, the length of the optical path, the expected standard deviation and the refractive indexes (real and imaginary). There is also an option to choose a high and a low level for one of the last two parameters if their values cannot be exactly estimated.

Figure 7 shows a parameter diagram that was generated for suspended latex particles in the DQ_1-DQ_2 plane. Predefined parameters such as particle size range, effective refractive index (automatically calculated by the system) and wavelengths values are used to calculate theoretical values of DQ_1 and DQ_2 by Eq. 24 These calculated values are plotted as curves in this DQ_1-DQ_2 plane. The numbers displayed on multiple positions of the curves correspond to the range of particle diameters selected for the calculation of the dispersion quotients. The curves have different shapes depending on calculated values DQ_1 and DQ_2. The shape diversity reflects the fact that parameters diagrams are specific to the type of particles, effective refractive index, medium and selected standard deviation of the size distribution.

Measured particle diameters are calculated from experimental dispersion quotients obtained after the light attenuation of the three laser wavelengths. These experimental DQ_1 and DQ_2 values are inserted in the parameter diagram leading to the display of several data points $X(DQ_1;DQ_2)$. X values are also generated at a speed of 1Hz during the measurement. The measured data points (Figure 7) are a direct indication of the measurement accuracy i.e. a measurement is considered accurate when X points are positioned on the theoretical curves during the measurement duration. This indicates that experimental dispersion quotients are in good agreement with the calculated ones. When data points are plotted outside the curves, this can be mainly explained by non adequate values chosen for the parameters described above in the text. The main advantage of such diagram is that it shows online the measurements accuracy and reliability without any need for measurement calibration by standard particles. OMT is an absolute measurement technique which does not allow any calibration.

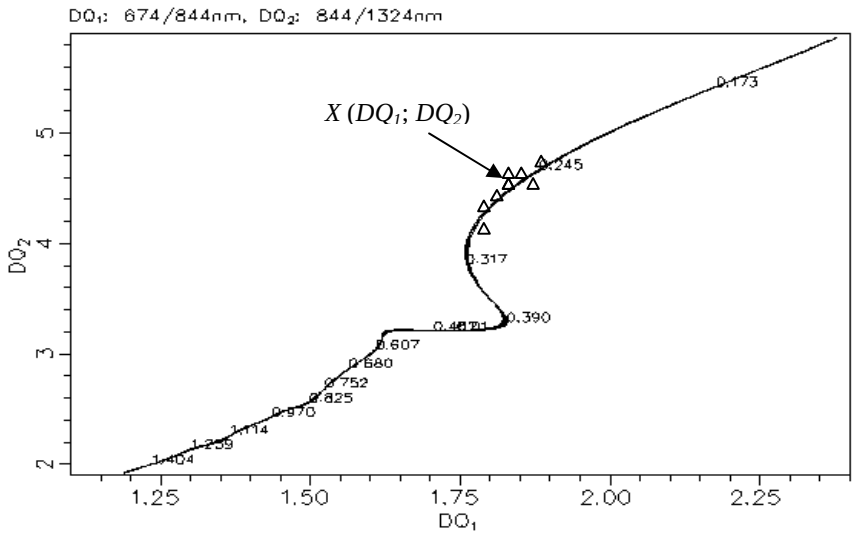

Figure 7. Parameter diagram generated for latex particles in suspension. Theoretical values of DQ_1 and DQ_2 calculated by Eq.24 are gathered and plotted as curves with values of particle size ranges. Data points $X(DQ_1,DQ_2)$ the experimental dispersion quotients obtained after light attenuation, are a direct probe of the measurement accuracy when they are positioned on the theoretical curves.

3. Off-line hyphenation of SdFFF with OMT

By hyphenating a size separation technique such as SdFFF with OMT, it is possible to determine the mean sizes of the eluted fractions and/or the mean size of the whole injected particulate sample. A comparison can be established between both mean sizes obtained by FFF equations [21, 90] and OMT. This hyphenation shows that the separation occurred in the FFF normal mode. It determines also the average size of particulate species when their density value, required for size calculation by FFF equations, is unknown. The first successful off-line hyphenation SdFFF-OMT is made and the obtained results are presented in this report.

Material and methods

1. SdFFF system

All FFF systems consist of a pump, an injection system, a separation channel and a detector. The whole system can be compared to a liquid chromatography device where the column is replaced by the channel. Figure 8 shows an FFF separation system. The pump generates the flow of the carrier liquid in the system. Sample injection is carried out by an injection valve placed between the pump and the channel. At the channel outlet the separated components pass through the detector measuring the elution signals, called fractograms.

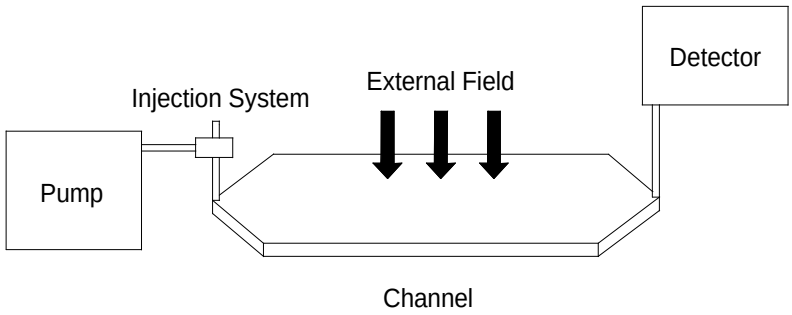

Figure 8. Schematic description of an FFF system.

The SdFFF separator (Figure 9) used in this research work is home-made and it has been already technically described [22-25, 34, 37, 38]. The separation channel is made up of two polystyrene plates, one described as the depletion wall and the other called the accumulation wall, separated by a Mylar band in which the channel is cut. Each channel is characterized by a specific length, width and thickness. Various channel dimensions were used according to the type of particulate species characterized in this work. The system void volume, which includes the connection tubing, injection and detector volumes, is usually measured using non retained solutes such as acetone 1% (v/v). The polystyrene plates with the Mylar band are sealed into a centrifuge basket (rotor bowl). Two rotating seals, drilled to allow the external diameter Peek® tubing to fit in, are used to permit the mobile phase to flow along the rotating axis into the channel. The types of

pumps, injection devices and detectors used are mentioned in the applications presented further in this report.

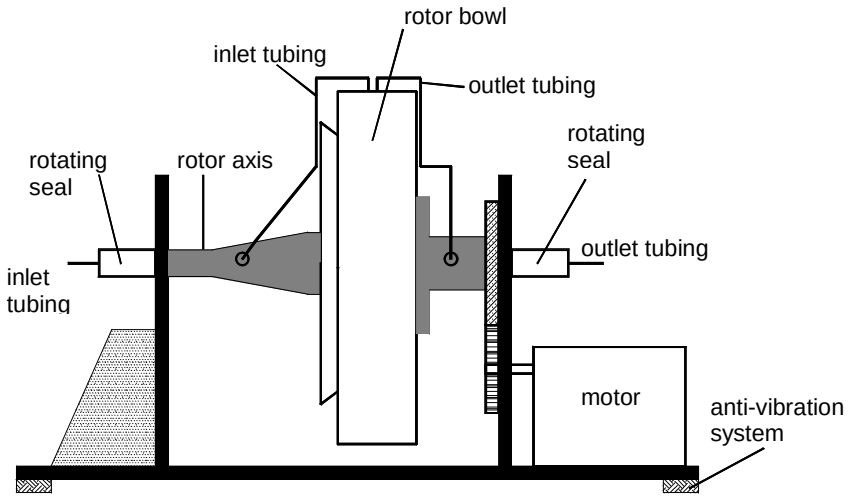

Figure 9. Schematic representation of the SdFFF separator with its different components. The rotor bowl is connected mechanically to an electrical engine that assures the proper spinning. The separator is installed on a mechanical support equipped with anti-vibration material to limit the system vibration while running.

2. Channel and rotor bowl

The channel is cut out of a plastic (Mylar) sheet of defined thickness as shown in Figure 10. The channel ends are V-shaped. The liquid penetrates into the channel at the end of one of the triangles and flows out of the channel at the other end. This shape prevents eddy flow in the channel. The Mylar sheet is clamped between two polystyrene plates, representing the channel walls. Polystyrene was chosen for two reasons: i) it is relatively inert with liquids mainly consisted of distilled water; ii) it is a flexible material able to mold the walls to the form of the rotor bowl.

Figure 10. Channel cut out of a Mylar® spacer.

Two holes are drilled in the polystyrene plates to let the carrier liquid flow in the channel through the Peek® tubing directly connected to the accumulation wall. Two channels are drilled through the wall of the rotor bowl to allow the Peek® tubing to fit in. The polystyrene plates with the Mylar band are clamped into the bowl (centrifuge basket) by means of a mechanical device which pushes the channel out against the inner surface of rotor wall as schematically shown in Figure 11. The channel is forced against this wall by screwing down the inner metallic cone and thus forcing the tripartite outer cone against the channel wall. This rotor bowl has to fulfill three requirements: i) guarantee the channel tightness; ii) enable the carrier phase to flow in and out of the channel; iii) it needs to be exactly equilibrated to prevent an increase of its moment of inertia. The higher the moment of inertia or the mass of the bowl, the more energy is needed to spin the bowl.

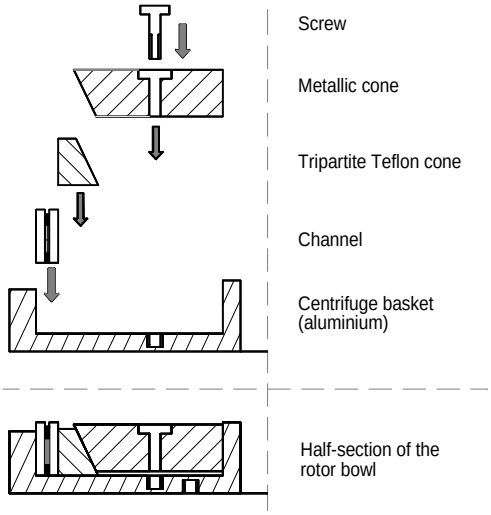

Figure 11. Section view of the rotor bowl: channel clamping system inside the rotor bowl.

The SdFFF separator (Figure 9) is installed on a mechanical support equipped with anti-vibration material to limit the system vibration while running. However, the vibration remains considerably important when the rotation speed is over 800 rpm. This fact is of a great inconvenience when higher rotation speeds are required for the separation of light colloids like soot particles analyzed in *Manuscript III*. The vibration can also cause the damage of the rotating seals (Figure 9) by reducing their shelf life. The reason for an increasing vibration with an increasing rotation speed is mainly due to an unbalance in

the weight distribution of the rotor bowl. In fact, when the rotor bowl is fully mounted (with the channel and polystyrene plates, the metallic and tripartite Teflon cones with screws), a weight unbalance was discovered by placing the rotor on a wheel balance. This unbalance is obtained between the front and back sides of the rotor bowl. The front side is heavier because the heavy parts like the metallic and the tripartite Teflon cones are sealed on the front side of the bowl (Figure 12). As a result, the rotation of the rotor bowl is not exactly perpendicular to the rotational axis because of the deviation of the gravity center. Thus, the system is subject to an increasing vibration with an increasing rotation speed.

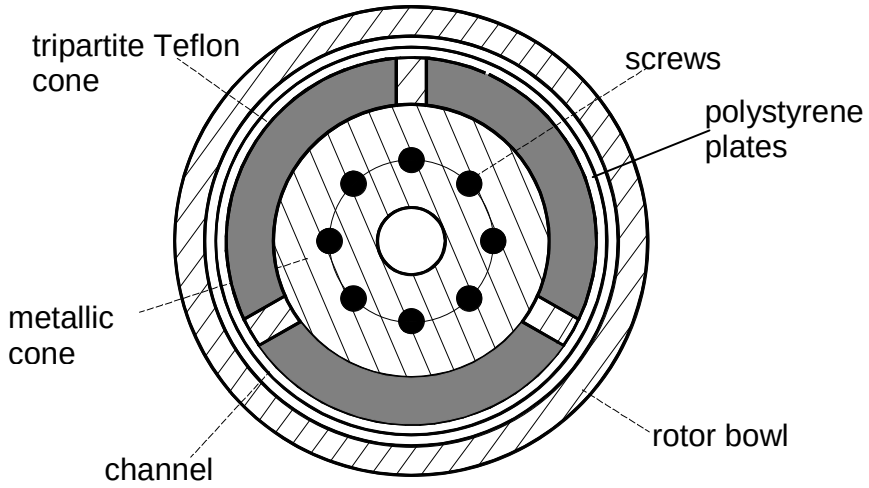

Figure 12. Front side of the rotor bowl with the sealed components: channel and polystyrene plates, metallic and tripartite Teflon cones, screws.

A possible way of circumventing this problem is by equilibrating the back side of the rotor. Therefore, a drainage of 0,5 cm breadth and 1 cm depth was made covering the whole perimeter of the rotor back side as shown in Figure 13. Small aluminum cubes (around 50 g each) were then fixed inside the drainage and positioned in a way to equilibrate both sides of the rotor. After this procedure, the vibration was reduced by 95%. The number of vibrations has been detected by an accelerator (Robert Bosch GmbH, Plochingen, Germany) equipped with a vibration sensor. The rotor was tightly positioned on the accelerator during the vibration measurements. A comparative diagram (Figure 14) of the number of vibrations per second versus the rotation speed shows the difference before and after the equilibration. The vibration was highly influenced by the increase of the rotation speed before the equilibration. However, it was considerably

reduced when the bowl was equilibrated and it even reached a steady state after 1500 rpm which allows a smoother rotation at high speeds and thus, a longer shelf life for the rotating seals.

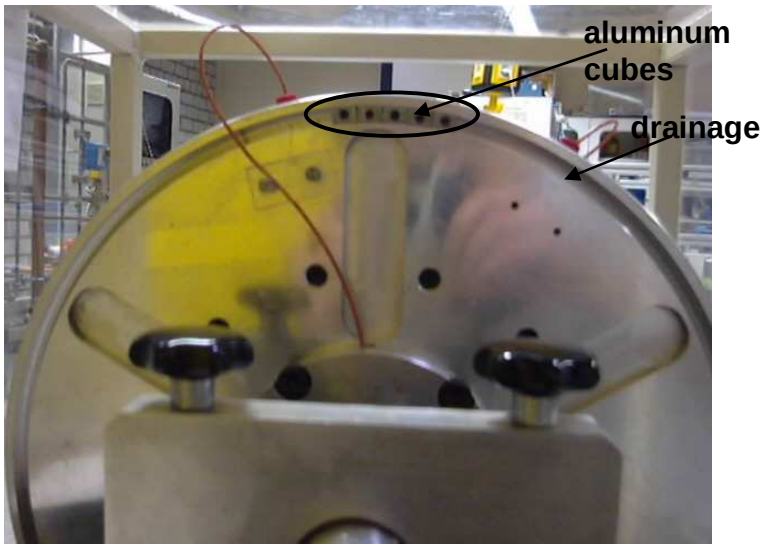

Figure 13. Back side of the rotor bowl with the drainage containing the aluminum masses.

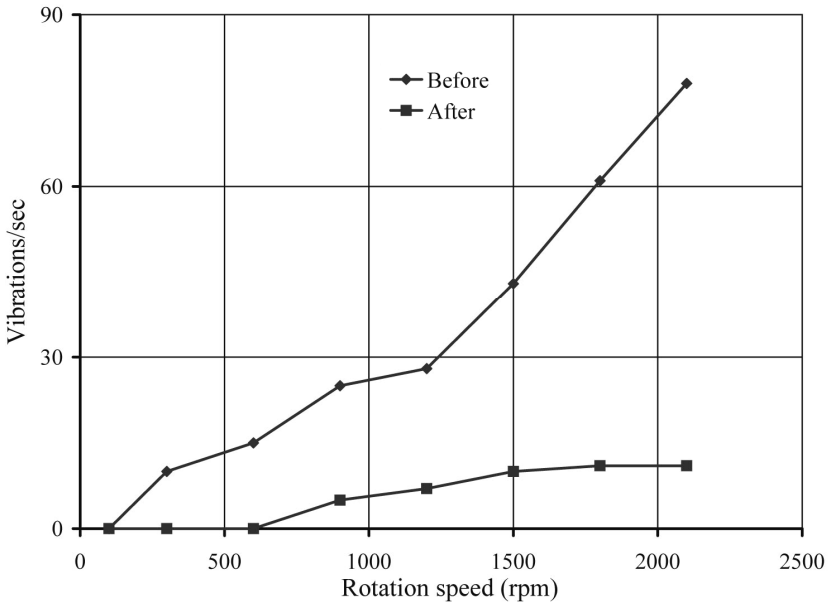

Figure 14. Comparative diagram of the number of vibrations/sec versus the rotation speed before and after the bowl equilibration.

3. Channel sealing procedure

The channel sealing procedure is more complicated than it was described in the previous section. Once the Mylar band (in which the channel is cut) is sealed in the centrifuge basket by means of the two flexible polystyrene plates, the relative flexibility of such system may produce channel geometry deformations which must be controlled.

A particular procedure is therefore necessary to seal the channel without deforming it. At first, the channel in the centrifuge basket is lightly pre-sealed mechanically to avoid leaks and the channel volume is controlled with acetone via an HPLC injector. If a proper sealing is performed, the acetone elution profile must comply two characteristics: its elution volume must correspond to the geometrical channel void volume (5% error tolerated) and the peak profile must be monomodal (chromatographic like). If discrepancies appear in terms of volume or peak shape, the sealing must be reprocessed. However, solutes with high diffusion coefficients do not sign alone a proper sealing which must be controlled using monodisperse standard latex beads as shown in Figure 15 in the case of the sealing procedure of an 80µm thick channel. According to the latex particle size (7µm) versus the channel thickness (80 µm), they were eluted according to the steric hyperlayer mode. Due to their relative great size compared to the channel thickness, their elution, at a given flow rate and low external field, is associated with high retention ratio which decreases with a field increasing intensity. When these monodisperse latex beads are eluted in this channel (not completely properly sealed), it is observed that latex peak profiles appear monomodal at high retention ratio (a, b, c, d) while with increasing external fields, elution profiles are completely deformed and appear multimodal (e,f,g,h).

There is therefore a go- and – back sealing procedure which leads to the elution pattern shown in Figure 16. It is observed that the void volume of the carrier liquid containing the surfactant is eluted with a remarkable monomodal gaussian profile. The intermediate field intensity corresponding to the Figure 15 (d, e) transition leads therefore to latex particle monomodal elution profiles analogous to those already described in the literature. Measured void volumes are in agreement with the parallelepiped geometrical volume of the channel. Therefore, it can be stated that this channel is properly sealed. However, as

shown in Figure 16, the elution performed in identical conditions was not reproducible. The cause of the lack in reproducibility is due to the necessity of a channel surface pretreatment which is explained in *Manuscript IV*.

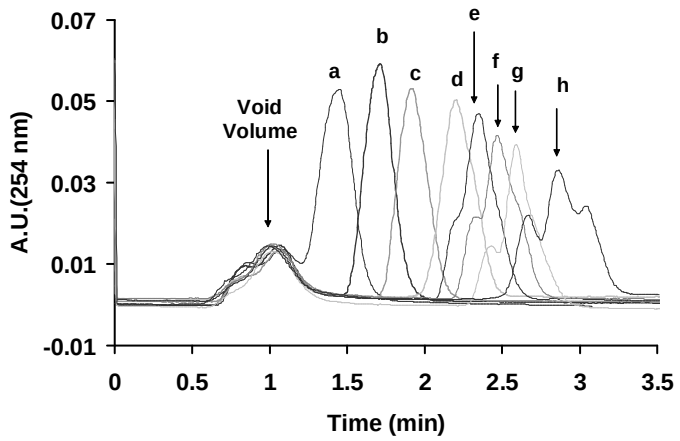

Figure 15. Improper sealing at accurate void volume. Example with 7µm Duke latex beads. Mobile phase composition: FL70/Water 0.1%(w/v). Measured flow rate: 0.98 mL/min. Rotation speed (rpm): a(187), b(250), c(315), d(445), e(508), f(571), g(634), h(756). Flow and field established injection procedure of a 20µL, 0.02% latex suspension in mobile phase.

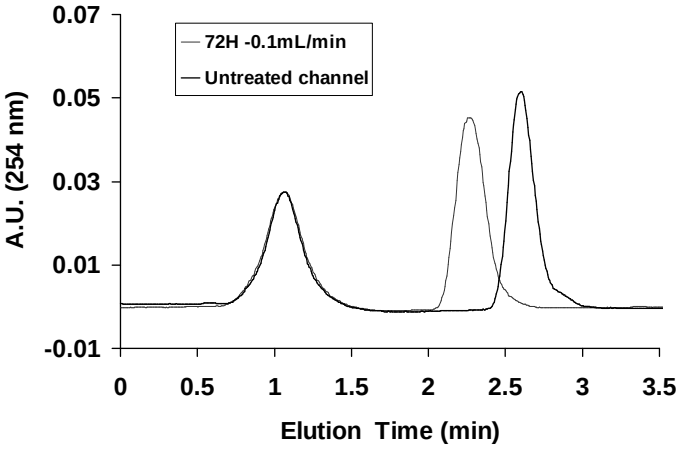

Figure 16. Properly sealed channel. Sample characteristics and injection procedures described in Figure 15. Rotation speed: 436.5 rpm. Measured flow rate:0.95 mL/min. Channel/mobile phase equilibration procedure: channel is flowed with mobile phase at low flow rate for 72H.

4. Field programming

There is a limitation in FFF when analyzing samples with very broad size distributions. The main problem is that to obtain an efficient separation of components with small size and to separate them from the void volume, a high external field (sedimentation field in case of SdFFF) is needed. However, the high sedimentation force will lead to very high elution times and poor detectability for sample components with larger size as they will be forced very close to the accumulation wall. In the worst case, they may be virtually immobilized on the accumulation wall due to the field intensity. This problem is solved by using a programmed field that starts the elution at a high sedimentation field suitable for components of smaller size after which the field is decayed over time, allowing the larger components to be eluted under the effect of a weaker field. In consequence, the elution times are reduced and the detectability is improved, especially for larger components in a broad distributed sample. Normally, the field decays according to some mathematical function. Various functions have been used for FFF subtechniques: linear [91, 92], exponential [93] and power programmed decays [94]. For each field decay, parameters like the initial field strength, relaxation time (the time during which the flow is stopped for letting the particles attend their equilibrium position in the thickness of the channel) and predecay time must be set depending on some particle characteristics such as size and density in case of SdFFF.

A three-phase engine (Carpanelli, Bologna, Italy) used for spinning the rotor bowl is controlled by an automation module composed of an inverter unit (KEB, Barntrup, Germany) connected to a programmable logic controller (PLC) step 5 device (Siemens, Karlsruhe, Germany). The PLC is used to program and store field decay sequences. Once programs are built and tested, they are enabled on a home made control box containing six function buttons. By pressing one of these, a specific programmed sequence is activated by sending appropriate analog signals to the KEB inverter (input voltage capacity around 10V) which allows the three-phase engine to perform the requested field decay. The rotation speed is monitored on-line during the run by means of a digital tachometer type RM-1501 (Prova instruments, Taiwan) via infrared link and connected to a central monitoring computer which acquires also analog input data coming from the

detector. Furthermore, this monitoring computer controls the output frequency of the KEB inverter by setting the maximum rotation speed of the three phase engine.

Among all field decays, the exponential one was applied for all SdFFF separations in this work because of the restriction in time to develop the field programming in order to start the applications. Moreover, developing such mathematical field decays with the available material requires both skill and time The exponential decay approach was first introduced by Kirkland et al [95] and it proved its effectiveness in the separation of broadly distributed samples. Figure 17 shows an example of a complete rotation speed curve performed according to an exponential decay. It was acquired on-line during the program execution. This curve is divided into three parts. The first one is the acceleration phase for reaching the maximum rotation speed set for the measurement. The second phase is the stabling of the speed at the maximum selected value for a certain period of time called relaxation time. The final phase is when the speed begins to decay exponentially performing predecay steps. For more information about this topic, the reader is referred to *Annex I* where he will find all details on the programming set up and the way the exponential decays were built.

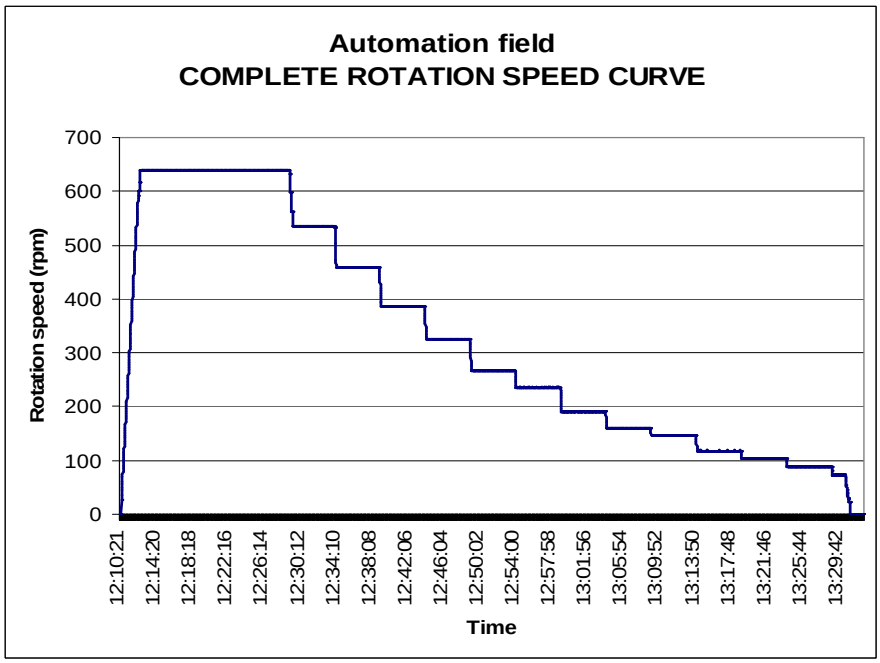

Figure 17. On-line curve of the rotation speed decay according to an exponential function.

5. Data acquisition system

A data acquisition system was developed for detection and integration of elution signals generated by the SdFFF system. This project took part in this thesis as a practicum work done by a formal master student. An adequate detector was needed to complete the instrumentation of the SdFFF system before starting the applications. The purpose of this work came after the purchase of a Postnova UV/Vis detector type S3120 (Postnova, Landsberg/Lech, Germany). The package hardware/software was over the fixed budget. Therefore, only the hardware was purchased and the manufacturer provided us with the necessary elements to develop our proper acquisition system. The idea to build a home made acquisition system seemed interesting and affordable. Furthermore, the necessary tools needed for this kind of project are available such as LabVIEW, a graphical programming environment (National Instruments Inc., USA) and different accessories like computers and multimeters. The LabVIEW version used is the 5.1 one.
It is built in a user friendly way and designed to fulfill the requirements of FFF due to its multiple features. It can be easily configured to run with all types of UV/Vis detectors. A main window leads the user to other sub windows presenting different system functions. It is also an open system where it is possible to load data from external files (acquired by other data acquisition systems) with ASCII characters in order to integrate the signals. Baseline corrections with peak smoothing techniques [96] and several parameter calculations can be executed such as peak statistical moments [97], exponentially modified Gaussian (EMG) constant, B/A ratio and many others. Help functions for each parameter, containing short definitions, are also available. The desired parameters results are saved under TXT files that contain all calculated values with peak data and they can be easily converted to excel. The system is adapted to the user needs as it can be saved under newer LabVIEW versions and more features can be added. A complete description about the data acquisition system can be found in *Annex II*.

6. OMT unit

OMT unit is developed by Wizard Zahoransky KG (Todtnau, Germany) and it is commercially available. This system is suitable to resolve in-line steady state and transient processes in aerosols and suspensions. It is able to monitor processes where particles at medium to high concentrations are involved. It can be applied in research areas to study particle reactions where no sampling is feasible or where the time resolved analysis of transient processes is of interest. Figure 18 shows the schematic of the presented particle measurement unit. The sensor head contains three laser diodes of different wavelengths (674, 844 and 1324 nm in its standard version) which are combined in one focused beam [82, 87]. The light is released at the measurement location and directed through the particle collective by the optics of the emitter part of the sensor head. On the other side of the measurement volume, the attenuated light beam is collected and directed to a photo-detector which is in the receiving part of the sensor head. The spectral attenuation of the three wavelengths is captured by the detector. Despite the time consuming calculation of the extinction coefficients Q_{ext} in Eq. 23 and 24 over the whole diameter spectrum by the Mie theory, a fast algorithm was developed to allow the on-line monitor display of the measurement data. Two parameters "measured diameter" and "volume concentration C_V" are displayed in operator's selected time intervals. The internal data acquisition rate is in the kHz range. The final displayed data points represent the average data values over the selected on-line time intervals, e.g. at a speed of 1 Hz. These data are additionally saved for later detailed post analysis and documentation.

For suspended particles, two optical cuvettes of 1 cm optical path length are used with different volume capacities: 2 ml and 160 µL for complete sample and fraction measurements respectively.

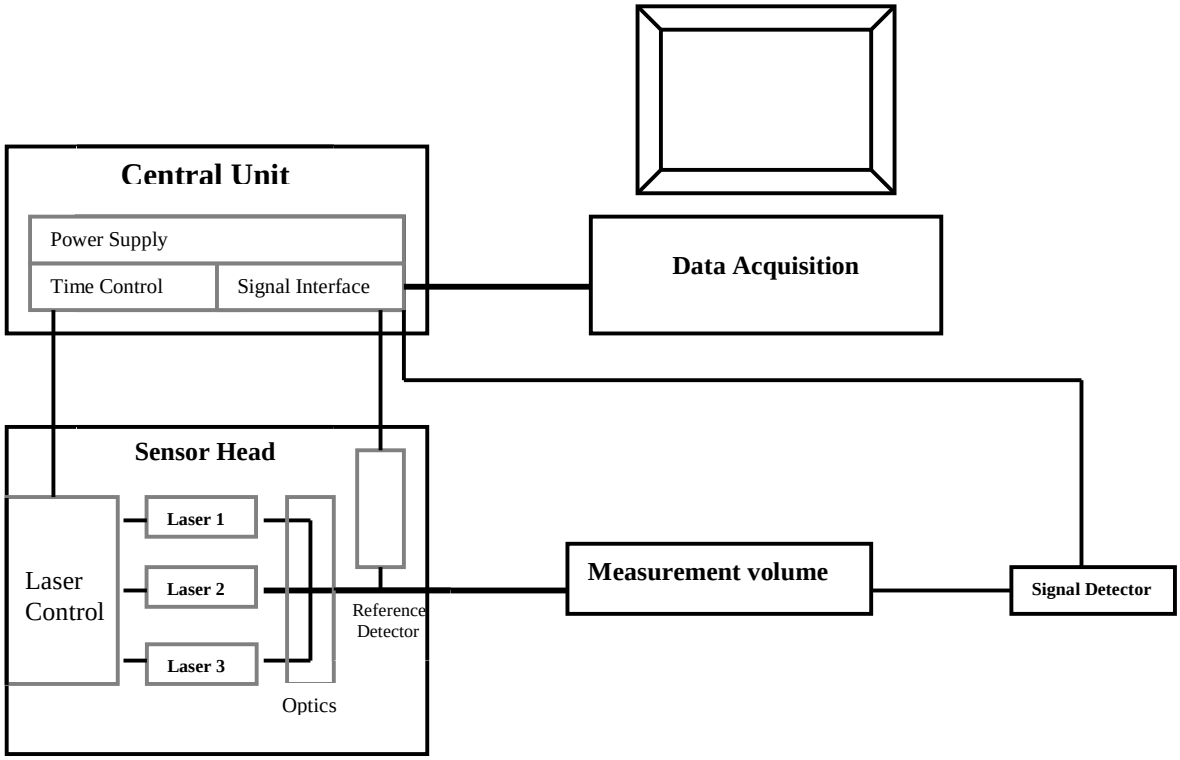

Figure 18. Schematic representation of the OMT measurement unit. The components are described in text.

Results and discussion

1. OMT-PCS-SEM comparative analysis of latex and oxide particles (Manuscript I)

The performance of OMT is evaluated in size characterization of suspended particle systems of different complexity in comparison to other known techniques like photon correlation spectroscopy (PCS) based on the diffusion coefficient measurement [98-100] and scanning electron microscopy (SEM) considered as a direct technique that provides images of particles from which the size of individual particles can be measured. Two types of particulate species with increasing complexity were selected: spherical latex particles having a narrow size distribution and oxide particles known for their broad distribution and shape irregularities. All particles were suspended in doubly distilled water containing 0.1% Sodium Dodecyl Sulfate (SDS), used as dispersing agent. 0.005% (w/w) of ZrO_2 and TiO_2 colloidal suspensions were prepared. The latex particles were diluted approximately 200 times. The latex average particle sizes were only given by the provider and the resulting sizes obtained by OMT and PCS showed good agreement with the provider's size values. Both techniques are accurate in size determination of narrow distributed particulate samples with well defined spherical shapes. The average sizes of both oxide particles obtained by OMT correlated also well with the ones given by PCS. However, some discrepancies were found with SEM resulting sizes which were higher than the ones obtained by OMT and PCS. This led to the conclusion that the increase in mean size by image analysis was most probably caused by the drying process. Morphological tools of the SEM image analysis could be less reliable when applied to samples having broad distributions and irregular shapes as observed for oxide particles in Figure 19. Therefore, the OMT and PCS size measurements are considered to be more accurate in the characterization of oxide colloidal samples. The reader is referred to *Manuscript I* further in this report for a complete description of this study.

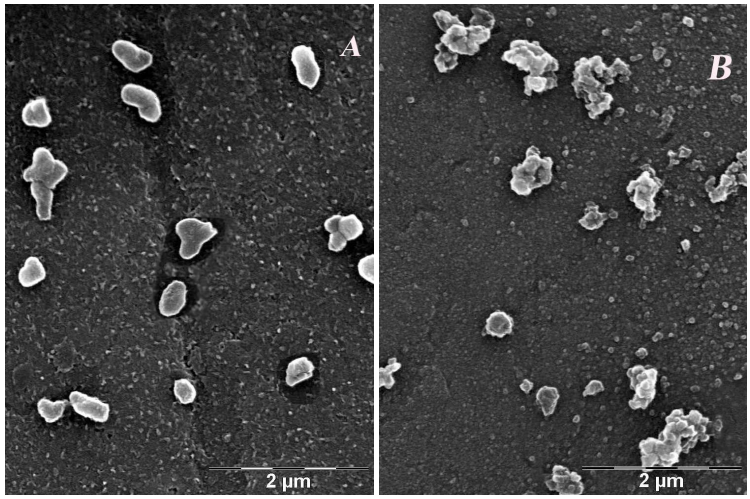

Figure 19. Electron microscopy profiles of TiO_2 (A) and ZrO_2 particles (B). Associated photo black lines used to calibrate each slide correspond to 2 µm.

2. SdFFF-OMT-SEM analysis of oxide particles (Manuscript II)

The topic of *Manuscript II* is the off-line hyphenation of SdFFF with OMT tested on oxide particles. By hyphenating SdFFF with OMT, it is possible to determine the mean particle sizes of time dependent eluted fractions. For this purpose, two types of oxide particles were selected: zirconium (ZrO_2) and titanium (TiO_2) oxides. 0.5% (w/w) colloidal suspensions were prepared in the carrier liquid composed of a doubly distilled and deonized water containing 0.1% (w/w) SDS (an anionic surfactant). High sample volumes (100 µL) were injected with medium suspension concentrations (0.5%) in order to generate a signal-to-noise ratio as large as possible compatible with accurate peak profile characteristics measurements and to provide enough amounts of particles for accurate electron microscopy (EM) size analysis without affecting the separation mechanism [101] due to intensive particle-particle and particle-wall interactions. Stop flow injections of the crude samples followed by exponential field gradients led to characteristic unimodal profiles. Figure 20 shows the TiO2 separation profile obtained after an exponential field decay. The time, needed for the particles to attend their equilibrium position in the thickness of the channel, called stop flow or relaxation time, was set to 15 min. The particles were injected in the channel at 0.2 ml/min flow rate.

During this period, the sedimentation field was fixed to a constant value G_0=17.1*g* (332.94 rpm) and then decreased exponentially with a predecay time of 2.5 min until it reached a final field strength of 2.56*g* (128.46 rpm). After reaching 2.56*g*, the field was kept constant till a baseline was reached. The elution flow rate was 1.5 ml/min. The separation time was ~ 39 min.

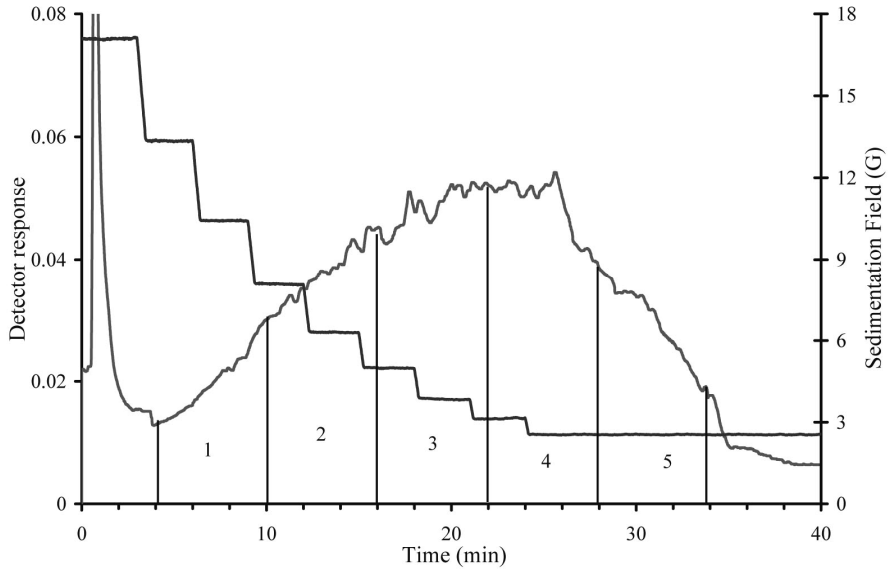

Figure 20. SdFFF fractogram of TiO_2 using UV/VIS detection. Exponential field decay acquired on-line during elution. Elution times of the 5 (6 min) collected fractions.

The other ZrO_2 elution profile is presented in *Manuscript II*. From the elution profiles, five fractions of identical volume (9ml) and collection time (6 min) were collected from each fractogram at different elution times. Fractions were then submitted to size analysis by SEM and OMT. SEM is used as a comparative technique to assess the accuracy of the size measurements and confirm the FFF selective separation of oxide particles. The mean sizes were also determined using FFF equations [21, 90] assuming a known and constant particle density. The size values obtained by SdFFF, OMT and SEM were in reasonable agreement showing that a size dependant separation occurred according to the normal elution mode assuming a constant density over the whole particle population. The sizes obtained by OMT and SEM slightly exceeded the ones calculated by FFF equations. The cause of this increase cannot be clearly justified because it is not only related to particle aggregation caused by the fraction sampling procedures (drying process for SEM and

concentration for OMT) applied before each measurement but also to different sizing approaches.

3. SdFFF-OMT-SMPS analysis of automobile soot particles (Manuscript III)

Particulate emissions generated by combustion can cause serious health problems by penetrating and delivering coated chemicals into human respiratory systems [55, 56]. Diesel engines are considered to be the major source of particulate emission. There are two types of diesel engines: light duty (LD) 4 cylinder engines used for passengers cars and heavy duty (HD) engines used in buses, trucks, construction equipments etc. The particulate matter (PM) in automobile exhaust is mostly fine carbonaceous particles (soot) that are coated with a mixture of various toxic chemicals such as polycyclic aromatic hydrocarbons (PAH). Soot particles have irregular shapes (usually in chain forms) formed by aggregation of several primary spherical particles [57]. The potential of SdFFF for size analysis of diesel soot particles has already been shown [102-104].

The PM emitted from a light duty (LD) Volkswagen (VW) diesel engine running at different engine speed and torque levels, is analyzed for mean size determination by programmed SdFFF and OMT. Results from both SdFFF and OMT are compared with those obtained from an online-scanning mobility particle sizer (SMPS). A study on soot sampling procedure for FFF and OMT analysis revealed a considerable influence of the surfactant concentration and the sonication amount on the mean size. An increase in the surfactant concentration from 0.01 to 0.1% (w/w) resulted in a decrease in the retention time and the mean particle size. An increase in the sonication from 10 to 110 min resulted in a more significant decrease in the retention time and the mean particle. After these findings, all collected samples were prepared by doubly distilled and deionized water containing 0.1% (w/w) SDS as a surfactant and they were sonicated for 90 minutes before SdFFF analysis. In this way, a good estimation of the particle size is assured to be obtained by FFF sizing equations and OMT. Fractions from soot fractograms in Figure 21 were collected at the peak maximum and they were submitted for OMT size analysis. The mean diameters obtained were used for the density calculation needed for the mean size determination by FFF equations.

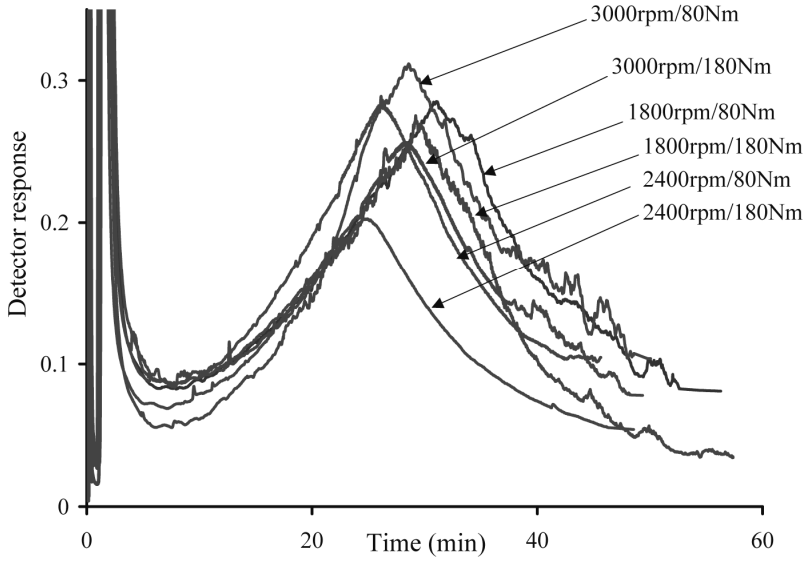

Figure 21. SdFFF elution profiles of collected soot samples. Elution conditions: initial field strength, 600*g* (1972 rpm); final field strength, 29.60*g* (439 rpm); predecay time, 5 min; stop flow time, 15 min; flow rate, 1.2 ml/min; sonication time, 90 min. Fractions collected at peak maximum for OMT size measurements.

An average density value of 1.73 g/cm^3 is obtained and applied for size determination of soot samples by FFF equations. For OMT and SdFFF, the size variation at different engine points is found to be more related to the variation in the collected PM amount that influenced the mean size due to the variable particle concentration in suspension. Therefore, the size variation obtained by SdFFF and OMT cannot be descriptive of the real size variation at different engine points because of the sample preparation procedure. A better estimation of this variation is given by on-line techniques like SMPS. For SMPS, the mean particle size seems to increase with an increasing torque at a constant engine speed. SMPS shows also a decrease in the mean size with an increasing engine speed at a constant torque level. A comparative diagram (Figure 22) shows the mean particle sizes obtained by the three techniques. A complete description of this study is available in *Manuscript III* included further in the report.

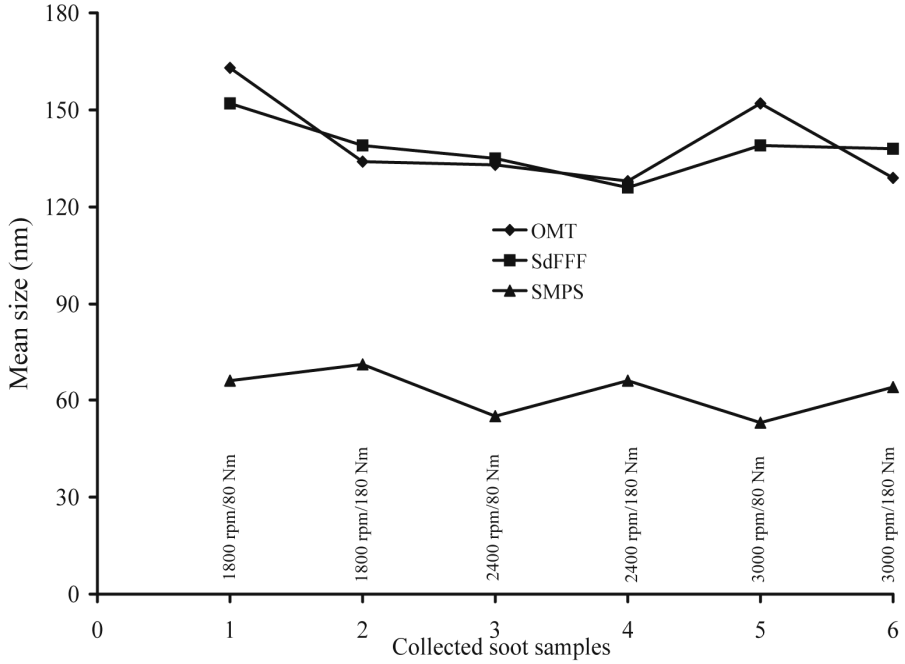

Figure 22. Mean sizes of soot particles emitted at different engine points determined by three different sizing techniques: OMT, SdFFF and SMPS.

4. Fast hyperlayer SdFFF separation (Manuscript IV)

The topic of *Manuscript IV* is to describe an advanced concept for SdFFF hyperlayer separation of micron sized species by using channels of reduced thickness which aims are to reduce the channel void volume, dilution factor, as well as elution time and mobile phase consumption. Therefore, several instrumental modifications on the classical field flow fractionation instrumentation and working conditions were performed. The modifications are: (i) the sample is introduced in the FFF separation system by means of a chromatographic injection loop when both the flow and the external field are established; (ii) in contrast with the commercially available instrumental set up used in SdFFF, the FFF channel inlet tube is connected to the accumulation wall of the channel; (iii) channels of reduced thickness are used to enhance the effect of the lifting forces as well as to reduce the elution time and volume. These modifications brought to the SdFFF system were investigated on standard latex micron particles. These spheres are considered to be monodisperse due to their low CV. All elutions were performed on the

flow mode i.e. the sample was introduced in the FFF system once the field and flow are established. Therefore, the separation process was very analogous to the ones performed in chromatography, simplifying considerably the operating conditions. This was made possible by means of a low volume tubing and mostly because the inlet tubing emerged in the channel via the accumulation wall. In this work, the methodology for channel installation is described on a 80 µm thick channel. At first, it must be properly sealed into the centrifuge basket to avoid leakage. A good sealing is performed when the elution volume corresponds to the geometrical channel void volume and the elution peak has to have a monomodal gaussian like profile. After sealing, a channel surface pretreatment is done by the use of FL70, a known surfactant for latex beads dispersion. It is composed of a mixture of ionic and non ionic surfactants. It was found that polystyrene channel walls need to be conditioned by the carrier containing the surfactant before any sample elution. Results showed that after 72 Hours of channel conditioning, a considerable shift was obtained in the retention ratio of the 7 µm latex beads elution profiles. Such phenomena can be interpreted by possible surfactant/wall interactions that lead to a shift in the retention time. A remarkable reproducibility (Figure 23) in terms of retention and peak profiles characteristics was also observed. However, the peak intensities were relatively different and furthermore, a peak release is observed at the end of the elution sequence due to the external field stop that released remaining trapped particles on the accumulation wall. Each elution was performed in less than 4 minutes. One of the characteristics of the hyperlayer elution mode is the retention dependence on the field intensity, and flow rate. Besides, It was proved that channel wall properties and carrier liquid composition influenced the retention when identical field intensity, flow rate and surfactant concentration were used.

To test the separation potential of channels with reduced void volumes, several particle mixtures were prepared. Fractograms obtained demonstrated the capacity of such channels in particle separation at specific field and flow conditions. For all elutions, a common separation procedure was applied. It consisted of two steps, the first one emphasizes the determination of an appropriate external field intensity while the second step is linked to an optimal flow rate. Figure 24 shows the potential of both 100 and 80 µm thick channels in a size dependent separation of a mixture of 5 and 7 µm latex

particles having different size polydispersities. Fractograms were obtained with almost analogous retention ratios but with different field/flow elution conditions. It is observed that latex beads resolution is maximized with the thinner channel because of the lower dilution factor that gave a more intense signal, and a reduced elution volume. Such results clearly sign the fact, that if particle populations only different in size are to be separated according to their size, the thinner channel generates the higher selectivity.

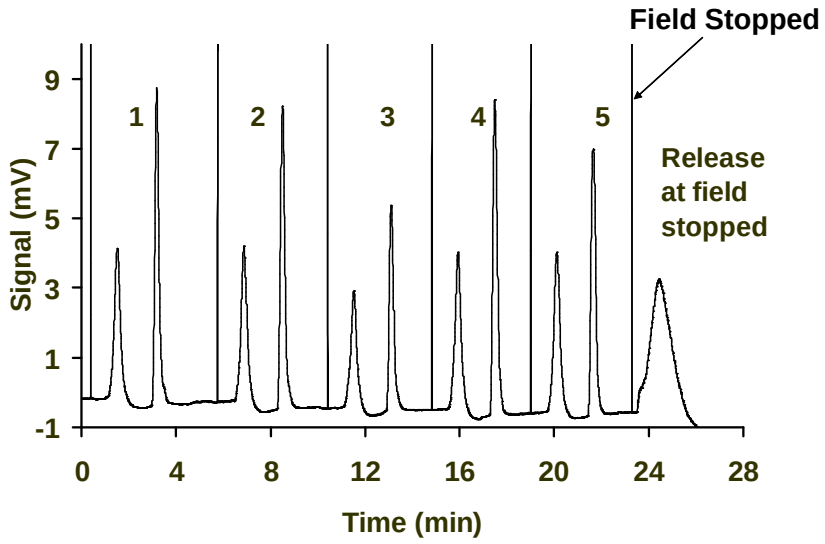

Figure 23. Elution reproducibility of the 7 µm latex beads. Mobile phase composition: FL70/Water 0.1% (w/v). Rotation speed: 436 rpm. Measured flow rate:0.95 mL/min.

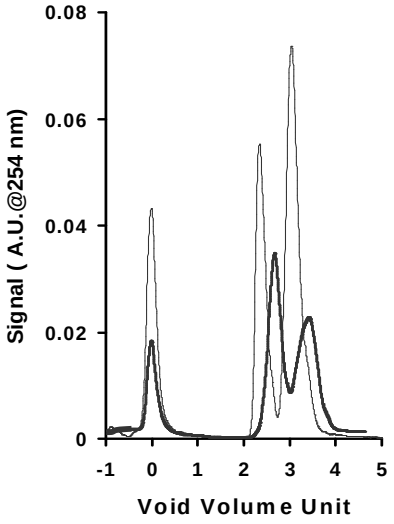

Figure 24. Retention ratio dependent fractograms of 5 & 7 µm latex particles in 80 (I) and 100 (II) µm thick channels. (——) correspond to channel I. (▬▬) correspond to channel II. Elution conditions: Channel I: 0.8 mL/min, 550 rpm; Channel II: 1.6 mL/min, 757 rpm.

Conclusion and perspectives

The performance of our SdFFF system has been investigated on different particulate species. From the investigations it has been demonstrated that such biocompatible [22, 24, 25, 34, 37, 38] system is well suited to be used in different applications either for the analysis of colloids or the separation of micron sized species. The fractograms demonstrated that this system reached a high performance level and it is at least equivalent to other laboratory or commercial SdFFF devices.

OMT has been introduced in this report as a technique for size measurement of suspended particles. Its applicability was first investigated on suspended particles of different complexity such as latex and oxide colloids. Its accuracy has been demonstrated when compared to other known techniques like PCS and SEM. After this introductive study on OMT, the off-line hyphenation with SdFFF was established. Its utility was to be evaluated in size analysis of fractions collected from exponentially programmed SdFFF separation of oxide colloids. The collected fractions were also analyzed by SEM, known to be an effective sizing technique for collected fractions with reduced polydispersity [23]. The mean particle sizes of fractions were also calculated by FFF related equations [21, 90] assuming a known and constant particle density. A good agreement was obtained in the end confirming the FFF size dependant separation according to the normal elution mode. For size analysis of soot particles, the hyphenation served as an indirect technique for the calculation of the particle density by determining the mean particle size of collected fractions at peak maximum. Size values obtained by SdFFF and OMT were compared to those measured by SMPS. The discrepancies in results are related to the measuring modes: SMPS is an on-line measurement technique while SdFFF and OMT are off-line techniques that require sample preparation before the analysis.

At the end, an advanced concept for SdFFF hyperlayer separation of micron sized species has been described. It aims to reduce the channel void volume, dilution factor, as well as elution time and mobile phase consumption. For this purpose, several modifications were made on the classical FFF instrumentation such as introducing the sample directly on the accumulation wall when both flow and field are established. The reduction of the channel thickness enhances the effect of the lifting forces and lowers the elution time and volume.

The SdFFF separation of colloids requires long elution times even with field programming operations and the size determination requires the density of particles to be known. However, for the separation of micron sized species, the elution is much more faster when both field and flow are established. No solid hypothesis is yet developed to determine the particle size in the hyperlayer elution mode. The retention ratio is only partially explained by the steric-hyperlayer elution hypotheses and depends on the size, density, rigidity and shape of the particle. So far, the significance of each of these parameters can only be described in a qualitative way [41, 44, 47, 48].

The main advantages of OMT in the analysis of suspended particles are its fast and easy operation where no pre measurement calibration is needed to verify the accuracy of obtained results. The probable disadvantage of this technique is that potential users may have difficulties to present and understand the displayed data in particular when compared to PCS or others where the particle size distribution is given. OMT generates the average size over the entire population and displays the time resolved size and volume concentration profiles. Furthermore, this technique was so far mostly used for particle sizing in aerosols where the designer thought that the display of size versus time is more informative for on-line measurements of particle cloud emissions to detect size variations when experimental parameters [83, 84] are modified during operation.

After its first introduction by Giddings, SdFFF proved its great performance in the separation and characterization of different types of colloids [23, 26] and micron sized species [37, 38]. Despite its broad applicability and high separating effectiveness, the usage of SdFFF was limited due to some instrumentation problems that were found on the commercial system. Another obstacle that slowed the FFF development is the absence of a general established theory concerning the elution modes due to various factors like the particle shape and fluid dynamics. Even if the sedimentation field is the most uniform and easiest to control among other external fields applied, it still lacks an application area of its own because of the absence of a commercial system specially dedicated to an application domain. The more established and wide spread separation techniques are continued to be used even in applications where SdFFF has proved to be at least suitable or even more suitable. However, The efforts and the promising results obtained by Cardot et al. [22-25, 34, 37], in combination with a more user-friendly SdFFF instrumentation,

can change this situation and put SdFFF in a future competitive position with the other known separation techniques. New SdFFF systems are currently under development and they will be adapted according to specific application domains like cell and colloidal separations. What is new about this system is its rotor bowl and rotation seals designs. The rotor bowl can be easily mounted and dismounted without removing other joint parts like bearings or mechanical links. The rotating seals are newly designed to support high rotation speeds and flow rates. The problems related to leakage are solved and the applicability is expected to be broadened in the separation of smaller or lighter particles in the colloidal range by generating high rotation speeds. Concerning the coupling of OMT to SdFFF, the promising results are motivating even if the concept is still at its early state. The on-line hyphenation is currently under development as it seems much more interesting where the SdFFF system can be directly linked to the OMT unit and thus, the peak signal can be directly converted to a time resolved size distribution profile according the three wavelengths approach. The main obstacle that is preventing the on-line hyphenation is the high dilution factor in the channel volume that reduces considerably the signal to noise ratio. This problem is being solved by studying the increase of the signal with an increasing optical path length according to Bouguer's law previously mentioned.

References

[1] GIDDINGS J. C. The conceptual basis of field-flow fractionation. J. Chem., 1973, 50, p. 667-669.

[2] GIDDINGS J. C. A new separation concept based on a coupling of concentration and flow nonuniformities. Sep. Sci., 1966, 1, p. 123-125.

[3] GIDDINGS J. C. Nonequilibrium theory of the field-flow fractionation. J. Chem. Phys., 1968, 49, p. 81-85.

[4] GIDDINGS J. C. Field flow fractionation : Analysis of macromolecular, colloids, and particulate materials. Science, 1993, 260, p. 1456-1465.

[5] GIDDINGS J.C., MYERS M. N., CALDWELL K. D. Field-flow fractionation: methodological and historical perspectives. Sep. Sci. Technol., 1981, 16, p. 549-575.

[6] SCHIMPF M. E. Advances in field-flow fractionation for polymer analysis. Trends Polymer Sci., 1996, 4, 4, p. 114-121.

[7] CALDWELL K. D. Field-flow fractionation. Anal. Chem., 1988, 60, p. 959A-971A.

[8] KIRKLAND J. J., DILKS C. H. Flow field-flow fractionation of polymers in organic solvents. Anal. Chem., 1992, 64, 22, p. 2836-2840.

[9] MYERS M. N., CALDWELL K. D., GIDDINGS J.C. A study of retention in thermal field flow fractionation. Sep. Sci., 1974, 9, p. 47-70.

[10] PASTI L., ROCCASALVO S., DONDI F., et al. High temperature thermal field flow fractionation of polyethylene and polystyrene. J. Polym. Sci. : Part B. Polym. Phys., 1995, 33, p. 411-416.

[11] CALDWELL K. D., GAO Y. S. Electric field flow fractionation in particle separation. 1. Monodisperse standards. Anal. Chem., 1993, 65, p. 1764-1772.

[12] LITZEN A., WAHLUND K. G. Zone broadening and dilution in rectangular and trapezoidal asymmetrical flow field-flow fractionation channels. Anal. Chem., 1991, 63, 10, p. 1001-1007.

[13] CARLSHAF A., JÖNSSON J.-Å. Gradient elution in hollow-fibre flow field-fractionation. J. Chromatogr., 1988, 461, p. 89-93.

[14] RESCHIGLIAN P., RODA B., ZATTONI A., et al. High performance, disposable hollow fiber flow field-flow fractionation for bacteria and cells. First application to deactivate Vibrio cholere. J. Sep. Sci., 2002, 25, p. 490-498.

[15] SCHIMPF M. E., CALDWELL K. D., GIDDINGS J. C. Field flow fractionation handbook. Wiley-interscience, Inc, New York, 2000, 592 p.

[16] CÖLFEN H., ANTONIETTI M. Field-flow fractionation techniques for polymer and colloid analysis. Springer- Verlag Berlin Heidelberg, 2000, 187 p.

[17] CARDOT P. J. P., GEROTA J., MARTIN M. Separation of living red blood cells by gravitational field-flow fractionation. J. Chromatogr., 1991, 568, p. 93-103.

[18] CARDOT P. J. P., LAUNAY J.-M., MARTIN M. Age-dependent elution of human red blood cells in gravitational field-flow fractionation. J. Liq. Chrom. Rel. Technol., 1997, 20, p. 2543-2553.

[19] SANZ R., TORSELLO B., RESCHIGLIAN P., et al. Improved performance of gravitational field-flow fractionation for screening wine-making yeast varieties. J. Chromatogr. A, 2002, 966, p. 135-143.

[20] URBÀNKOVÀ E., VACEK A., CHMELIK J. Micropreparation of hemopoietic stem cells from mouse bone marrow suspension by gravitational field-flow fractionation. J. Chromatogr. B, 1996, 687, p. 449-452.

[21] GIDDINGS J. C. Measuring colloidal and macromolecular properties by FFF. Anal. Chem., 1995, 67, p. 592A-598A.

[22] ASSIDJO E., CHINEA T., DREYFUSS M. F. Validation procedures of sedimentation field flow fractionation techniques for biological applications. J. Chromatogr. B, 1998, 709, p. 197-207.

[23] CARDOT P. J. P., RASOULI S., BLANCHART P. TiO_2 colloidal suspension polydispersity analysed with sedimentation field flow fractionation and electron microscopy. J. Chromatogr. A, 2001, 905, p. 163-173.

[24] BATTU S., ROUX A., DELBASEE S., et al. Sedimentation field-flow fractionation device cleaning, decontamination and sterilization procedures for cellular analysis. J. Chromatogr. B, 2001, 751, p. 131-141.

[25] CARDOT P. J. P., BATTU S., SIMON A., et al. Hyphenation of sedimentation field flow fractionation with flow cytometry. J. Chromatogr. B, 2002, 768, p. 285-295.

[26] GIDDINGS J. C., MYERS M. N., MOON M. H., et al. Particle separation and size characterization by sedimentation field flow fractionation. In: T. Provder (Eds.), Particle size distribution II: Assessment and characterization., 1991, ACS Symp. Series No. 472, American chemical society, Washington, DC, p. 198-213.

[27] KARAISKAKIS G., GRAFF K. A., CALDWELL K. D., et al. Sedimentation field-flow fractionation of colloidal particles in river water. Int. J. Environ. Anal. Chem., 1982, 12, p. 1-15.

[28] CALDWELL K. D., KARAISKAKIS G., MYERS M. N., et al. Characterization of albumin microspheres by sedimentation field-flow fractionation. J. Pharm. Sci., 1981, 70, p. 1350-1360.

[29] CALDWELL K. D., KARAISKAKIS G., GIDDINGS J. C. Characterization of T4D virus by sedimentation field-flow fractionation. J. Chromatogr., 1981, 215, p. 323-332.

[30] YONKER C. R., CALDWELL K. D., GIDDINGS J. C., et al. Physical characterization of PBCV virus by sedimentation field flow fractionation. J. Virol. Methods, 1985, 11, p. 145-156.

[31] KIRKLAND, J. J., YAU W. W., SZOKA F. C. Sedimentation field flow fractionation of liposomes. Science, 1982, 215, p. 296-298.

[32] SCHALLINGER L. E., GRAY J. E., WAGNER L. W., et al. Preparative isolation of plasmid DANN with sedimentation field-flow fractionation. J. Chromatogr., 1985, 342, p. 67-77.

[33] SCHALLINGER L. E., YAU W. W., KIRKLAND, J. J. Sedimentation field-flow fractionation of DNA's. Science, 1984, 225, p. 434-437.

[34] SANZ R., CARDOT P. J. P., BATTU S., et al. Steric-hyperlayer sedimentation field flow fractionation and flow cytometry analysis applied to the study of Saccharomyces cervisiae. Anal. Chem., 2002, 74, p. 4496-4504.

[35] MOZERSKY S. M., CALDWELL K. D., JONES B. E., et al. Sedimentation field-flow fractionation of mitochondrial and microsomal membranes from corn roots. Anal. Biochem., 1988, 172, p. 113-123.

[36] SCHALLINGER L. E., ARNER E. C., KIRKLAND J. J. Sixe distribution of cartilage proteoglycans determined by sedimentation field flow fractionation. Biochim. Biophys. Acta., 1988, 966, p. 231-238.

[37] GUGLIELMI L., BATTU S., LE BERT M., et al. Mouse embryonic stem cell sorting for the generation of transgenic mice by sedimentation field flow fractionation. Anal. Chem., 2004, 76, p. 1580-1585.

[38] BATTU S., COOK-MOREAU J., CARDOT P. J. P. Sedimentation field-flow fractionation: methodological basis and applications for cell sorting. J. Liq. Chrom. Rel. Technol., 2002, 25, p. 2193-2210.

[39] JANCA J. Field-flow fractionation: analysis of macromolecules and particles. Chromatographic Science Series, 1988, 39, Marcel Dekker, New York.

[40] GIDDINGS J. C. Unified separation science. Wiley, New York, 1991.

[41] GIDDINGS J. C., MYERS M. N. Steric field-flow fractionation: a new method for separating 1-100 µm particles. Sep. Sci. Technol., 1978, 13, p. 637-645.

[42] MOON M. H., GIDDINGS J. C. Extension of sedimentation/steric field-flow fractionation into submicron range: size analysis of 0.2-15 µm metal particles. Anal. Chem., 1992, 64, p. 3029-3037.

[43] RESCHIGLIAN P., TORSI, G. determination of particle size distribution by gravitational field-flow fractionation: dimensional characterization of silica particles. Chromatographia, 1995, 40, p. 467-473.

[44] CALDWELL K. D., NGUYEN T. T., MYERS M. N., et al. Observations on anomalous retention in steric field-flow fractionation. Sep. Sci. Technol., 1979, 14, 10, p. 935-946.

[45] RESCHIGLIAN P., MELUCCI, D., TORSI, G. Experimental study on the retention of silica Particles in gravitational field-flow fractionation; effects of the mobile phase composition. J. Chromatogr. A., 1996, 740, p. 245-252.

[46] GIDDINGS J. C. Hyperlayer field-flow fractionation. Sep. Sci. Technol., 1983, 18, p. 765-773.

[47] WILLIAMS P. S., KOCH T., GIDDINGS J. C. Characterization of near-wall hydrodynamic lift forces using sedimentation field-flow fractionation. Chem. Eng. Comm., 1992, 111, p. 121-147.

[48] PAZOUREK J., CHMELIK J. Optimization of the separation of micron-sized latex particles by gravitational field-flow fractionation. Chromatographia, 1993, 35, p. 591-596.

[49] McNEIL L. E., FRENCH R. H. Multiple scattering from rutile TiO_2 particles. Acta Mater., 2000, 48, p. 4571-4576

[50] MORITZ T., WERNER G., TOMANDL G., et al. Sintered ceramics for sub-micron filtering. Sci. Forum, 1999, 308-311, p. 884-889.

[51] SPANOS N., GEORGIADOU I., LYCOURGHIOTIS A. Study on colloidal suspension stability. J. Colloid Interf. Sci., 1993, 156, p. 374-378.

[52] BACH G., ABELARD P., BLANCHART P. Electrical conductivity and dielectric dispersion phenomena of concentrated TiO_2 suspensions. J. Colloid Interf. Sci., 2000, 228, p. 423-427.

[53] WALSH M. Serious pollution by particulate emissions generated by combustion. SAE NA Techn. Pap. Ser., 1998, No: 1998-01-186.

[54] DOCKERY M. An association between air pollution and mortality in six U.S. cities. The new England Journal of Medicine, 1993.

[55] FARTHING W. E. Soot effect on the human respiratory system. Environ. Sci. Technol., 1982, 16, p. 237A- 244A.

[56] CUDDIHY R. G., GRIFFITH W. C., McCLELLAN R. O. Inhaled components into the human respiratory system. Environ. Sci. Technol., 1984, 18, p. 14A-21A.

[57] ISHIGURO T., TAKATORI Y., AKIHAMA K. Microstructure of diesel soot particles probed by electron microscopy: First observation of inner core and outer shell. Combust. Flame, 1997, 108, p. 231-234.

[58] CARRARO E., LAURA L. A., FERRERO C., et al. J. Environ. Pathol. Toxicol. Oncol., 1997, 16, p. 101-107.

[59] KERMINEN V.-M., MAEKELAE T. E., OJANEN C. H., et al. Characterization of the particulate phase in the exhaust from a diesel car. Environ. Sci. Technol., 1998, 31, p.1883-1889.

[60] MARICQ M. M., PODSIADLIK D. H., CHASE R. E. Gasoline vehicle particle size distributions: comparison of steady State, FTP, and US06 measurements. Environ. Sci. Technol., 1999, 33, p. 2007-2015.

[61] THOMPSON G. H., MYERS M. N., GIDDINGS J. C. An observation of a field-flow fractionation effect with polystyrene samples. Sep. Sci., 1967, 2, p. 797-800.

[62] WEERS J. G., ARLAUKAS R. A. Sedimentation field-flow fractionation studies of Ostwald ripening in fluorocarbon emulsions containing two disperse phase components. Langmuir, 1995, 11, p. 474-477.

[63] ATHANASOPOULOS A., KARAISKAKIS G. Potential barrier gravitational field-flow fractionation for the analysis of polydisperse colloidal samples. Chromatographia, 1995, 40, p. 734-736.

[64] BARMAN B. N., GIDDINGS J. C. Separation of colloidal latex aggregates by cluster mass and shape using sedimentation field-flow fractionation with steric perturbations. Anal. Chem., 1995, 67, p. 3861-3865.

[65] KARAISKAKIS G., KOLIADIMA A., KLEPERNIK K. Estimation of polydispersity in polymers and colloids by field-flow fractionation. Colloid Polym. Sci., 1991, 269, p. 583-589.

[66] MORI Y., KIMURI K., TANIGAKI M. Influence of particle-wall and particle-particle interactions on retention behavior in sedimentation field-flow fractionation. Anal. Chem., 1990, 62, p. 2668-2672.

[67] HOYOS M., MARTIN M. Retention theory of sedimentation field-flow fractionation at finite concentrations. Anal. Chem., 1994, 66, p. 1718-1730.

[68] KIRKLAND J. J., REMENTER S. W., YAU W. W. Time-delayed exponential field-programmed sedimentation field flow fractionation for particle-size-distribution analyses. Anal. Chem., 1981, 53, p. 1730-1736.

[69] ZATTONI A., MELUCCI D., GIANCARLO T., et al. Quantitative analysis in field-flow fractionation using ultraviolet-visible detectors: an experimental design for absolute measurements. J. Chromatogr. Sci., 2000, 38, p. 122-128.

[70] RESCHIGLIAN P., MELUCCI D., ZATTONI A., et al. Quantitative approach to field-flow fractionation for the characterization of supermicron particles. J. Microcol. Sep. 1997, 9, 7, p. 545-556.

[71] OPPENHEIMER L. E., SMITH G. A. Sedimentation field-flow fractionation of colloidal metal hydrosols. J. Chromatogr., 1989, 461, p. 103-110.

[72] SCHIMPF M. E., WILLIAMS P. S., GIDDINGS J. C. Accurate molecular weight distribution of polymers using thermal field-flow fractionation with deconvolution to remove system dispersion. J. Appl. Polymer. Sci., 1989, 37, p. 2059-2076.

[73] KIRKLAND J. J., REMENTER S. W. Polymer molecular weight distributions by thermal field flow fractionation using Mark-Houwink constants. Anal. Chem., 1992, 64, p. 904-913.

[74] MARTIN M., HES J. On-line coupling of thermal field-flow fractionation with low-angle laser light scattering. Sep. Sci. Technol., 1984, 19, p. 685-709.

[75] THIELKING H., KULICKE W. M. On-Line coupling of flow field-flow fractionation and multiangle laser light scattering for the characterization of macromolecules in aqueous solution as illustrated by sulfonated polystyrene samples. Anal. Chem., 1996, 68, p. 1169-1173.

[76] ANDERSSON M., WITTGREN B., WAHLUND K. G. Accuracy in multiangle light scattering measurements for molar mass and radius estimations. Model calculations and experiments. Anal. Chem., 2003, 75, p. 4279-4291.

[77] WITTGREN B., WAHLUND K. G., ARFVIDSSON C., et al. Polysaccharide characterization by flow FFF-MALS. Initial studies of modified starches. Int. J. Polym. Anal. Charac., 2002, 7, p. 19-40.

[78] SCHIMPF M. E. Determination of molecular weight and composition in copolymers using thermal field-flow fractionation combined with voscosimetry. In: T. Provder (Eds.), Chromatographic characterization of polymers: hyphenation and multidimensional techniques., 1995, ACS, Washington, DC, p. 183-196.

[79] TAYLOR H. E., GARBARINO J. R., MURPHY D. M., et al. Inductively coupled-plasma-mass spectrometry as an element-specific detector for field-flow fractionation particle separation. Anal. Chem., 1992, 64, p. 2036-2041.

[80] HASSELÖV M., HULTHE G., LYVEN B., et al. Electrospray mass spectrometry as online detector for low molecular weight polymer separations with flow field-flow fractionation. J. Liq. Chromatogr. Rel. Technol., 1997, 20, p. 2843-2856.

[81] ANDERSSON M., WITTGREN B., WAHLUND K. G. Ultra high molar mass component detected in ethylhydroxyethyl cellulose cellulose asymmetrical flow field-

flow fractionation coupled to multiangle light scattering. Anal. Chem., 2001, 73, p. 4852-4861.

[82] NIKITIDIS M. S., KONSTANDOPOULOS A. G., ZAHORANSKY R. A., et al. Correlation of measurements of a new long optical path length particle sensor against gravimetric and electrical mobility based particle measurements in diesel exhaust. SAE NA Techn. Pap. Ser., 2001, No: 2001-01-73.

[83] ZAHORANSKY R. A., KERZENMACHER S., BENALI G., et al. Particle emissions of the Jing-Cast burner examined by multi-wavelength particle analyzer. SAE NA Techn. Pap. Ser., 2003, No: 2003-01-53.

[84] LAILE E., ZAHORANSKY R. A., MOHR M., et al. Optical on-line time resolved particle measurements in the exhaust gas of diesel engines for different test cycles. SAE NA Techn. Pap. Ser., 2003, No: 2003-01-56.

[85] PFEIFER U., ZARSKE S., SAMENFINK W., et al. Optical mutliple wavelength extinction technique applied to on-line measuring of diameter and volume concentration of particles in the exhaust gas of diesel engines. VDI Bericht, 1995, 1189, p. 285-300.

[86] SCHABER K., SCHENKEL A., ZAHORANSKY R. A. Drei-Wellenlangen-Extinktionverfahren zur Charakteriesung von Aerosolen unter industriellen Bedingungen. tm-Technisches Messen, 1994, 61, p. 295-300.

[87] WENDE B., LAILE E., ZAHORANSKY R. A., et al. On-line measurement of fog droplets in wet scrubbing processes. Chem. Eng. Technol., 2001, 24, p. 235-238.

[88] MIE G. Beiträge zur Optik trüber Medien, speziell kolloidaler Metallösungen. Annalen der Physik IV, 1908, 25, p. 377-445.

[89] Willeke K., Baron P.A. The scattering of light. New York: Van Nordstrand Reinhold, 1993.

[90] GIDDINGS J. C., YOON Y. H., CALDWELL K. D., et al. Nonequilibrium plate height for field-flow fractionation in ideal Parallel Plate Columns. Sep. Sci., 1975, 10, p. 447-460.

[91] KULICKE W. M., HEINS D., SCITTENHELM N. Determination of the absolute molar mass and particle size distribution of water-soluble cellulose and starch derivatives. Polym. Mater. Sci. Eng., 1998, 79, p. 427-428.

[92] THIELKING H., ROESSNER D., KULICKE W. M. On-line coupling of flow field-flow fractionation and multiangle laser light scattering for the characterization of polystyrene particles. Anal. Chem., 1995, 67, 18, p. 3229-3333.

[93] KIRKLAND J. J., DILKS C. H., REMENTER S. W., et al. Asymmetric-channel flow field-flow fractionation with exponential force-field programming. J. Chromatogr., 1992, 593, p. 339-355.

[94] BOTANA A. M., RATHANATHANOWONGS S. K., GIDDINGS J. C. Field-programmed flow field-flow fractionation. J. Microcol. Sep., 1995, 7, 4, p. 395-402.

[95] KIRKLAND J.J., YAU W. W., DOERNER W.A., et al. Sedimentation field flow fractionation of macromolecules and colloids. Anal. Chem., 1980, 52, p. 1944-1954.

[96] DYSON N. Chromatographic integration methods. The Royal Society of Chemistry, 1990, 160 p.

[97] OPPENHEIM A. V., SCHAFER R. W. Discrete-time signal processing. Pretince Hall, Inc., 1989, 220 p.

[98] PHILIES G. D. J. Anal. Chem., 1990, 62, p. 1049A-1055A

[99] BARTH H.G., SUN S. T. Particle size analysis. Anal. Chem., 1995, 67, p. 257R-272R.

[100] LEE S., RAO S. P., MOON M. H., et al. Determination of mean diameter and particle size distribution of acrylate latex using flow field-flow fractionation, photon correlation spectroscopy, and electron microscopy. Anal. Chem., 1996, 68, p. 1545-1549.

[101] WILLIAMS P. S., GIDDINGS M. C., GIDDINGS J. C. A data analysis algorithm for programmed field-flow fractionation. Anal. Chem., 2001, 73, p. 4202-4211.

[102] KIRKLAND J. J., LIEBALD W., UNGER K. K. Characterization of diesel soot by sedimentation field flow fractionation. J. Chromatogr. Sci., 1990, 28, p. 374-378.

[103] KIM W. S., PARK Y. H., SHIN J. Y., et al. Size determination of diesel soot particles using flow and sedimentation field-flow fractionation. Anal. Chem., 1999, 71, p. 3265-3272.

[104] KIM W. S., KIM S. H., LEE D. W., et al. Size analysis of automobile soot particles using field-flow fractionation. Environ. Sci. Technol., 2001, 35 , p. 1005-1012.

Manuscript I

Comparative size determination of latex and oxide particles by optical multiwavelength technique, photon correlation spectroscopy and scanning electron microscopy

James R. Kassab[1,2], Richard A. Zahoransky[2*], Philippe Blanchart[3], Dominique Clédat[1], Philippe J.P. Cardot[1]

1-Laboratoire de Chimie Analytique et de Bromatologie, Université de Limoges Faculté de Pharmacie, 2 Rue du Dr. Marcland, F-87025 Limoges, Cedex, France

2-International Quality Network, Nanoparticles and Bioparticles Project, University of Applied Sciences, Badstr. 24, D-77652 Offenburg, Germany

3-Groupement d'Etude des Matériaux Hétérogènes, Ecole Nationale Supérieure de céramique industrielle, 47 Avenue Albert Thomas, F-87025 Limoges, Cedex, France

*Corresponding author: Tel.: +49-781-205255; fax: +49-781-205242.

E-mail address: zahoransky@fh-offenburg.de

Abstract

Optical multiwavelength technique (OMT) is a newly introduced particle measurement method developed for suspensions and aerosols based on the Mie theory. It delivers in on-line/in-line mode the particle mean size and volume concentration over an entire particle population. Measurements were performed using suspensions of narrow polystyrene latex beads and polydisperse particulate matter such as oxide particles to show the accuracy of OMT in terms of size determination. Comparative measurements were performed by Coulter Sub-micron Particle Sizer (CSPS) that derives the particle size from particle diffusion coefficient measurements by photon correlation spectroscopy (PCS). The data displayed by both techniques is different: OMT unit determines time resolved profiles of particle size and volume concentration while CSPS provides the particle scattering intensity versus the size. Average particle sizes obtained by OMT and CSPS are in good agreement with size values given by the provider concerning latex particles. Certain discrepancies are observed when compared to scanning electron microscopy (SEM) for oxide particles. This is due to broad sample distributions and shape irregularities that affect negatively the accuracy in size determination by image analysis.

Keywords: Colloids; field flow fractionation; latex particles; optical multiwavelength technique; photon correlation spectroscopy; scanning electron microscopy; titanium oxide; zirconium oxide.

Manuscript II

Characterization of titanium and zirconium oxide colloids by off-line hyphenation of sedimentation field flow fractionation with optical multiwavelength technique

James R. Kassab[1,2], Richard A. Zahoransky[2], Philippe Blanchart[3], Philippe J.P. Cardot[1*], Bernd Spangenberg[2]

1-Laboratoire de Chimie Analytique et de Bromatologie, Université de Limoges Faculté de Pharmacie, 2 Rue du Dr. Marcland, F-87025 Limoges

2-Fachhochschule Offenburg, University of Applied Sciences, Badstr. 24, D-77652 Offenburg

3-Groupement d'Etude des Matériaux Hétérogènes, Ecole Nationale Supérieure de céramique industrielle, 47 Avenue Albert Thomas, F-87025 Limoges

*Corresponding author: Tel.: +33-5-55435857; fax: +33-5-55435859.

E-mail address: cardot@unilim.fr

Abstract

Optical multiwavelength technique (OMT) is a newly introduced particle measurement method developed for suspensions and aerosols based on the Mie Theory. It delivers in on-line/in-line mode the particle mean size and volume concentration over an entire particle population. Sedimentation Field Flow Fractionation (SdFFF) using the centrifugal force to operate, gained considerable success in the separation of particulate samples of colloidal size. The separation in FFF occurs according to size of particles for samples of uniform densities. The off-line hyphenation of SdFFF with OMT is established in this report for the characterization of titanium and zirconium oxide colloids. Time dependant eluted fractions are collected and submitted to OMT for size analysis. Results obtained by SdFFF and OMT are then compared to the particle size values of fractions determined by electron microscopy (EM). The accuracy of the size measurements is confirmed because of a good resulting agreement.

Keywords: Colloids; field flow fractionation; optical multiwavelength technique; scanning electron microscopy; titanium oxide; zirconium oxide.

Manuscript III

Size analysis of soot particles emitted from a light duty diesel engine using sedimentation field flow fractionation

James R. Kassab[1,2], Annett Wollmann[3], Richard A. Zahoransky[2], Michael Claussen[3], Philippe J.P. Cardot[1*]

1-Laboratoire de Chimie Analytique et de Bromatologie, Université de Limoges Faculté de Pharmacie, 2 Rue du Dr. Marcland, F-87025 Limoges

2-Fachhochschule Offenburg, University of Applied Sciences, Badstr. 24, D-77652 Offenburg

3-CUTEC Institut GmbH, Leibnizstr. 21 +23, D-38678 Clausthal-Zellerfeld

*Corresponding author: Tel.: +33-5-55435857; fax: +33-5-55435859.

E-mail address: cardot@unilim.fr

Abstract

Soot particles emitted from a light duty (LD) VW diesel engine running at different engine operating points (engine speed and torque) are analyzed for mean size determination using two off-line techniques: sedimentation field flow fractionation (SdFFF) and optical mutiwavelength technique (OMT), a newly introduced sizing technique for particles in suspension derived from a long path multi-wavelength extinction technique (LPME) used for size determination of particles in aerosols. Soot samples are prepared for FFF analysis. Optimized conditions for surfactant concentration and sonication time are applied as they revealed their effect on the mean particle size. The mean diameters determined by SdFFF show similar trends with those obtained from OMT. Data from SdFFF and OMT are also compared with those from an online-scanning mobility particle sizer (SMPS). The amount of particulate matter (PM) emitted is higher at low torque than that at high torque. The engine operating points (engine speed and torque) seem to affect differently the mean particle sizes measured by SMPS and SdFFF-OMT. The discrepancies between these techniques are mainly related to the required sample preparation procedure employed for SdFFF and OMT measurements. SMPS is an on-line technique that directly measures the size of soot particles.

Keywords: Field flow fractionation; online-scanning mobility particle sizer, optical multiwavelength technique, soot particles.

Manuscript IV

Fast “hyperlayer” separation development in sedimentation field flow fractionation using channels of reduced thickness.

James R. Kassab[1], Philippe J.P. Cardot[1*], Richard A. Zahoransky[2], Serge Battu[1]

1-Laboratoire de Chimie Analytique et de Bromatologie, Université de Limoges Faculté de Pharmacie, 2 Rue du Dr. Marcland, F-87025 Limoges, Cedex, France

2-International Quality Network, Nanoparticles and Bioparticles Project, University of Applied Sciences, Badstr. 24, D-77652 Offenburg, Germany

*Corresponding author: Tel.: +33-5-55435857; fax: +33-5-55435859.

E-mail address: cardot@unilim.fr

Abstract

Sedimentation field flow fractionation (SdFFF) can be used for micron sized separation using channels of reduced thickness which aims are to reduce the channel void volume, dilution factor, as well as elution time and mobile phase consumption. These goals are of major interest for SdFFF systems used, which have to be qualified using reference materials like controlled latex particles. The major price to be paid is mainly instrumental, that is to set up a parallelepiped channel and to reduce dramatically connecting tubing volumes, as well as to modify their position in the separator. It is demonstrated that micron sized latex particles can be separated in few minutes and they are eluted according to the qualitatively known “Hyperlayer elution mode”. Once the instrumentation is set, the separation scheme development uses two steps, the first one emphasizes the determination of an appropriate “external field intensity” while the second step is linked to an optimal flow rate. However depending on the composition of the mobile phase (surfactant type), the elution characteristics are modified as well as the recovery. The fractograms demonstrated that such biocompatible designed SdFFF system is at least equivalent to other laboratory or commercial SdFFF devices. In terms of sample injection procedure, the innovative use of inlet tubing linked to the FFF accumulation wall allows to avoid any primary relaxation step.

Keywords: Sedimentation field flow fractionation; latex particles; size polydispersity; tween.

Annex I

Field programming for sedimentation field flow fractionation

Omar Ignacio Valdés Solórzano[1], James R. Kassab[1,2]

1-Fachhochschule Offenburg, University of Applied Sciences, Badstr. 24, D-77652 Offenburg

2-Laboratoire de Chimie Analytique et de Bromatologie, Université de Limoges Faculté de Pharmacie, 2 Rue du Dr. Marcland, F-87025 Limoges

Abstract

If samples to be fractionated are very polydisperse, a high external field strength must be applied in order to separate the least retained particles. As a result, well-retained species leave the separation channel after an excessively long period. This problem is solved by gradually decreasing the field strength affecting the retained solute. In case of sedimentation field flow fractionation SdFFF, a second reason for applying field programming is to improve the detectability of the larger components. Normally, the field decays according to some mathematical function. Various functions have been used for FFF subtechniques such as linear, exponential, parabolic and power programmed decays. For each field decay, parameters like the initial field strength, relaxation time (the time during which the flow is stopped for letting the particles attend their equilibrium position in the thickness of the channel) and predecay time must be set depending on some particle characteristics like size and density in case of SdFFF. Among all field decays, the exponential one is selected in this project work. The programmed sequences are developed to provide the best possible approximation using a programmable logic controller (PLC).

Annex II

Data acquisition system for sedimentation field flow fractionation developed by LabVIEW© graphical programming language

César Ansgar de Juan Esteban[1], James R. Kassab[1,2]

1-Fachhochschule Offenburg, University of Applied Sciences, Badstr. 24, D-77652 Offenburg

2-Laboratoire de Chimie Analytique et de Bromatologie, Université de Limoges Faculté de Pharmacie, 2 Rue du Dr. Marcland, F-87025 Limoges

Abstract

A data acquisition system was developed for detection and integration of elution signals generated by the SdFFF system by means of LabVIEW© graphical programming language. It is built in a user friendly way and designed to fulfill the requirements of FFF due to its multiple features. It can be easily configured to run with all types of UV/Vis detectors. A main window leads the user to other sub windows presenting different system functions. It is also an open system where it is possible to load data from external files (acquired by other data acquisition systems) with ASCII characters in order to integrate the signals. Baseline corrections with peak smoothing techniques and several parameter calculations can be executed such as peak statistical moments, exponentially modified Gaussian (EMG) constant, B/A ratio and many others. Help functions for each parameter, containing short definitions, are also available. The desired parameters results are saved under TXT files that contain all calculated values with peak data and they can be easily converted to excel. The system is adapted to the user needs as it can be saved under newer LabVIEW versions and more features can be added.